NASA/TM–2019–220280

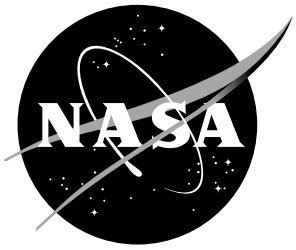

Indoor Ground Testing of a Small UAS Sense and Avoid Airborne Doppler Radar

George N. Szatkowski
Langley Research Center, Hampton, Virginia

Larry A. Ticatch, Christopher M. Morris, and Angelo A. Cavone
Analytical Mechanics Associates, Langley Research Center, Hampton, Virginia

May 2019

NASA STI Program. . . in Profile

Since its founding, NASA has been dedicated to the advancement of aeronautics and space science. The NASA scientific and technical information (STI) program plays a key part in helping NASA maintain this important role.

The NASA STI Program operates under the auspices of the Agency Chief Information Officer. It collects, organizes, provides for archiving, and disseminates NASA's STI. The NASA STI Program provides access to the NASA Aeronautics and Space Database and its public interface, the NASA Technical Report Server, thus providing one of the largest collection of aeronautical and space science STI in the world. Results are published in both non-NASA channels and by NASA in the NASA STI Report Series, which includes the following report types:

- TECHNICAL PUBLICATION. Reports of completed research or a major significant phase of research that present the results of NASA programs and include extensive data or theoretical analysis. Includes compilations of significant scientific and technical data and information deemed to be of continuing reference value. NASA counterpart of peer-reviewed formal professional papers, but having less stringent limitations on manuscript length and extent of graphic presentations.

- TECHNICAL MEMORANDUM. Scientific and technical findings that are preliminary or of specialized interest, e.g., quick release reports, working papers, and bibliographies that contain minimal annotation. Does not contain extensive analysis.

- CONTRACTOR REPORT. Scientific and technical findings by NASA-sponsored contractors and grantees.

- CONFERENCE PUBLICATION. Collected papers from scientific and technical conferences, symposia, seminars, or other meetings sponsored or co-sponsored by NASA.

- SPECIAL PUBLICATION. Scientific, technical, or historical information from NASA programs, projects, and missions, often concerned with subjects having substantial public interest.

- TECHNICAL TRANSLATION. English-language translations of foreign scientific and technical material pertinent to NASA's mission.

Specialized services also include organizing and publishing research results, distributing specialized research announcements and feeds, providing information desk and personal search support, and enabling data exchange services.

For more information about the NASA STI Program, see the following:

- Access the NASA STI program home page at `http://www.sti.nasa.gov`

- E-mail your question to `help@sti.nasa.gov`

- Phone the NASA STI Information Desk at 757-864-9658

- Write to:
  NASA STI Information Desk
  Mail Stop 148
  NASA Langley Research Center
  Hampton, VA 23681-2199

NASA/TM–2019–220280

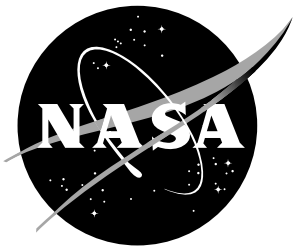

Indoor Ground Testing of a Small UAS Sense and Avoid Airborne Doppler Radar

George N. Szatkowski
Langley Research Center, Hampton, Virginia

Larry A. Ticatch, Christopher M. Morris, and Angelo A. Cavone
Analytical Mechanics Associates, Langley Research Center, Hampton, Virginia

National Aeronautics and
Space Administration

Langley Research Center
Hampton, Virginia 23681-2199

May 2019

Available from:

NASA STI Program / Mail Stop 148
NASA Langley Research Center
Hampton, VA 23681-2199
Fax: 757-864-6500

Abstract

The National Aeronautics and Space Administration's Unmanned Aircraft System (UAS) Traffic Management (UTM) project is researching prototype technologies needed to ensure safe integration of UAS operations into the National Airspace System (NAS). Within the UTM Concept of Operations, UAS would be equipped with on-board Sense and Avoid (SAA) technology to continually monitor for manned and unmanned aircraft in its vicinity while operating beyond visual line of sight in uncontrolled airspace. To support this effort, a candidate commercially available 24.5 GHz Doppler radar was selected and evaluated to determine if the technology could reliably support minimum requirements for SAA applications of small UAS (sUAS). Indoor ground tests were conducted inside the NASA Langley Research Center's Experimental Test Range (ETR) from a stationary platform to evaluate the Doppler radar performance characteristics and gain operational proficiency before the radar was authorized to transmit outdoors.

A high speed linear rail system was developed for the radar evaluation and was shown to be an effective method to generate Doppler radar targets of known radar cross section. The accuracy of the range and velocity reported by the radar was shown to be dependent on the Kalman filter state variance parameter settings. Antenna measurements were collected with the radar installed both on and off a sUAS to quantify the relative antenna gain, beam width and side lobe levels of the radar's Metamaterial Electronically Scanning Array (MESA) antennas at boresight and extreme field of view pointing vectors. The relative antenna gain measured 2.6 dB lower at extreme field view angles compared to the boresight radiation pattern.

Introduction

The NASA UTM project is conducting research to evaluate prototype technologies needed to safely integrate UAS operations into the NAS. Within the UTM Concept of Operations, UAS will be equipped with on-board Sense and Avoid (SAA) technology to continually monitor for manned and unmanned aircraft in its vicinity while operating beyond visual line of sight in uncontrolled airspace. Under this scenario, the sense and avoid sensor would relay the location and trajectory information of the airborne targets to the UAS ground control system to adjust the UAS vehicle heading or to enact an automatic contingency procedure to maneuver the UAS autonomously. The NASA developed SAA algorithm ICAROUS, (Independent Configurable Architecture for Reliable Operations of Unmanned Systems) has been designed to incorporate real time radar tracking data to execute autonomous maneuvers to eliminate potential airborne conflicts.

To support UTM goals and development of the ICAROUS SAA algorithm, a candidate sense and avoid 24.5 GHz Doppler radar marketed for UTM operations was operated to evaluate its capabilities to locate, track and alert the presence of airborne vehicles operating in the UAS's vicinity for the purpose of autonomous maneuvering. To develop the software required to ingest the radar track data into ICAROUS and to increase proficiency at operating the radar before it could be operated outdoors or flown on a UAS, performance verification assessments were conducted indoors at the NASA Langley Experimental Test Range (ETR). The ETR is a large compact range far field anechoic test facility used to characterize large space based antennas and other electromagnetic systems. The indoor radar assessments were designed to gain a better understanding of the radar's operational characteristics beyond the products technical specifications published and to build knowledge in programing the commands to control the radar.

Since the Doppler radar can only track targets that have greater than 0.455 meters per second relative radial velocity, a method to generate a Doppler target that could be detected and tracked inside the ETR was needed. To achieve this, a 5 m long high speed linear belt-drive actuator system was developed to translate a copper hemisphere along the linear rail. Four different sized metal hemispheres were tested independently on the linear rail to generate Doppler targets of varying radar signatures. The metal hemispheres were selected as the Doppler target since its radar signature is well established and its specular scattering characteristics eased target alignment issues. Measurement comparisons between the radar's recorded track data estimated radar cross section values from the various sized hemispheres with the known spherical specular radar cross section values provided additional insight into the relationship between the radar's state variance

software commands and the accuracy of the Kalman filter tracking algorithm.

Antenna measurements were collected to examine the performance of the radar's Metamaterial Electronically Scanning Array (MESA) antenna to maintain its gain and beam width specifications at extreme field of view pointing vectors. to quantify the transmitted radiation pattern from the MESA antenna. The measurements were acquired with and without the radar installed on a candidate UAS to verify that the radar's operational field of view was not impacted due to rotor motor line of sight blockage. New experimental methods were developed to achieve this assessment since proprietary restrictions on accessing the radar antennas prevented standard practice antenna measurements which incorporate a network analyzer to both transmit and receive the radiated signal. A spectrum analyzer was employed in the ETR data acquisition software to receive the radar's transmission to conduct the measurements. The gain of the antenna directly relates to the radar's detection range and a significant drop in gain over the radar field of view would limit the radar's ability to detect air traffic at those viewing angles.

Outdoor flight testing will be required to determine the maximum range a sUAS can be tracked, the lateral and vertical angular errors, rate of false and missed/late detections, and estimated distance at closest point of approach after an avoidance maneuver is executed. This last metric is directly impacted by sensor performance and indicates its suitability for the task. The main goal, at the conclusion of this effort is to determine if this radar technology can reliably support minimum requirements for SAA applications of sUAS.

Symbols & Acronyms

A/D	Analog to Digital
dBi	Decibels isotropic
dBm	Decibel power based on one milliwatt
dBsm	Decibels per square meter
ETR	Experimental Test Range
FMCW	Frequency Modulated Continuous Wave
HPBW	Half Power Beam Width
ICAROUS	Independent Configurable Architecture for Reliable Operations of Unmanned Systems
IF	Intermediate Filter
MESA	Metamaterial Electronically Scanning Array
msec	Milliseconds
NAS	National Airspace System
NASA	National Aeronautics and Space Administration
NITA	National Telecommunications and Information Administration
Range	Distance from Radar to Doppler Target
RCS	Radar Cross Section
RF	Radio Frequency
SAA	Sense and Avoid
sUAS	Small Unmanned Aircraft System
UTM	Unmanned Aircraft System Traffic Management
API	Application Programing Interface

Experimental Setup

The candidate UTM sense and avoid sensor selected for this research was a Frequency Modulated Continuous Wave radar with 120° azimuth and 80° elevation field of view operating at 24.55 GHz center frequency with a 45 MHz swept bandwidth. The radar transmits 2 watts of peak power thru a Metamaterial Electronically Scanning Array antenna oriented in horizontal polarization. The 22 dBi gain from the MESA antenna requires personnel to be at least 1 meter away from the active array to limit nonionizing radiation exposure. The radar physical dimensions are 18.7 cm x 12.1 cm x 4.1 cm and it weighs less than 820 grams making it well suited for installation on small UASs. A photograph of the radar is shown in Figure 1 and 2. The radar has independent transmit and receive antenna arrays divided by a small aluminum metal fence to reduce cross talk coupling. The radar firmware version 10 was used during this evaluation. Enhancements to improve the performance of the Kalman filter have been achieved in later firmware versions. Software 13 will be used to conduct the actual flight test experiments.

The radar is controlled using a command line interface API software called BNET thru an Ethernet TCP protocol. Scripting commands are used to establish the radars operational characteristics including the search and track fields of view, parameters to govern the tracking Kalman filter and data logging selections. Radar detections are generated every time the radar is able to detect a Doppler target. Detections may or may not turn into radar tracks depending on the radar masking settings defined in the startup script command.

The radar track and detection data packets are recorded in binary (.bin) files. By default, detection packets are transmitted at a rate of every beam step period, 6.72 msec, while Track data packets by default are transmitted every 4.98 Hz which gives about 210 msec between every update. The user cannot modify the Detection transmit rate, but the Track data transmit rate can be configured to transmit at the user specified track update rate in the range (0.0, 5.0) per second. In later firmware versions the update rate has increased to 10 Hz.

A Python script was developed to parse the radar generated detection.bin and track.bin files. The parser application opens the respective radar detection or track .bin files, parses the binary data found in these files, then stores the parsed information into new ASCII formatted .csv files that can be viewed and manipulated in common spreadsheet applications such as Microsoft Excel for future plotting and analysis. The parsed .csv files contain all variables found in the Track and Detection packets needed for analysis including x, y, z, coordinate locations, azimuth, elevation, and range coordinates, velocity, confidence level, estimated radar cross section (RCS), lifetime of the track and sample acquisition time. The parser also calculates two additional outputs used in the data analysis. The total velocity, which is calculated from the radar velocities given in x, y, and z coordinates provides a measure of direct correlation to the speed of the Doppler target regardless of direction. The relative recorded time from the first track point is also calculated to provide a standard time base between tracks and is used as the x-axis for the data plots. To expedite plotting and analysis of the .csv files, a LabVIEW based application was developed. The plotting routine retrieves individual data points assembled in detection and tracking .csv data files and automatically generates data plot curves viewable in Microsoft Excel. Data plots were created to display the radar tracking data's position, velocity and RCS versus time for the hemisphere Doppler targets.

The radar evaluation was conducted inside the NASA Langley ETR compact range anechoic chamber to enable the research team to gain valuable operational experience before the formal National Telecommunications and Information Administration (NITA) spectrum authorization was received to allow outdoor transmissions and operated on a sUAS. Operating the Doppler radar inside the ETR to evaluate its tracking performance created several unique challenges. Indoor testing of a Doppler radar is typically conducted using a Doppler radar target simulator. The simulator receives the radar's transmitted RF signal thru an antenna and adjusts the signal frequency to correlate with the desired simulated target velocity. The frequency adjusted signal is then transmitted back to the radar. The simulator approach would be expected to generate radar detections, but would not provide the target displacement needed to exercise the settings for the Kalman filter algorithm. To generate tracking data, a method to move a Doppler target at speeds greater than 0.455 m/s was needed. To maintain a probability of false alarm (PFA) of 1E-6 or in one in one million, the target's Doppler signature needs to be at least 13 dB above the surrounding range bins' stationary clutter. Each range bin spans a distance of 3.25 m. In addition, the default range mask setting of the Doppler radar prevents detection or track information from being reported in the first 19.5 m (6 range bins) from the radar aperture. The range mask is incorporated as a default parameter to prevent nearby targets from being tracked to enable the MESA more time to search for new potential tracks. To accommodate the minimum standoff distance of 19.5 m required between the radar and the Doppler target and to separate potential sources of stationary radar clutter, the radar was installed on a tripod in the ETR's second floor mezzanine looking into the back of the ETR anechoic chamber (see Figure 3). The radar search field of view was set of ±6° in azimuth and -12° to -28° in elevation to sweep across the desired search volume.

New hardware was developed to generate track data from Doppler radar targets moving at speeds greater than 0.455 m/s. A target translating back and forth on a 5 m high speed linear rail actuator was determined to be the most effective solution to generate repeatable track data. The Tolomatic B3W10 Linear Belt-Drive Actuator was purchased to translate a radar target at up to 5 m/s, well exceeding the minimum velocity of 0.455 m/s required for the radar to generate detections and tracks. Software code was developed in the "Kollmorgen Workbench" to interface with the Kollmorgen AKD Basic programmable servo drive motor to operate the rail. The software provided functionality to control the acceleration, velocity and travel distance of the Doppler target along the full length of the rail. The Doppler rail

system was mounted to the floor toward the back of the ETR. RF absorbing anechoic material was placed around the rail to reduce stationary ground clutter and ground bounce Doppler reflections. Figure 3 shows the basic physical arrangement between the radar and the rail.

To generate tracking data from Doppler targets with varying radar signatures, four different sized metal hemispheres with diameters of 3, 6, 8 and 12 in., shown in Figure 4, were mounted to the rail and measured independently. The metal hemisphere was selected as the Doppler target since its radar signature is well established and its specular scattering characteristics eased target alignment issues. The radar cross section of the 3, 6, 8 and 12 inch diameter hemispheres was calculated to be -23.4 dBsm, -17.39 dBsm, -14.89 dBsm and -11.37 dBsm respectively based on the specular return calculation for a hemisphere. Each hemisphere was translated on the rail for approximately 100 sec per test. Figure 5 shows the hemisphere mounting arrangement on the linear motion rail.

There are several parameters in the radar that a user can change to adjust detection and tracking performance. One such parameter is the "state variance" of the target. State variance is a measure of the expected maneuverability of a target and can be thought of as the average acceleration in units of meters per second squared. Matching the state variance parameters to the target's expected maneuverability will allow the Kalman filter to more accurately maintain a target's track during accelerated maneuvers. Increasing the state variance beyond the optimal setting will cause the accuracy of the reported track (position and velocity) to be diminished. Four tests were performed on each hemisphere to evaluate different Kalman filter state variance settings. The state variance command in this firmware version controls both the maneuvering and steady variance settings. For each hemisphere tested, the maneuvering and steady variance settings were made the same and set to either 0.1, 0.2, 0.5 or 1.0. The Kalman filter parameters provide the means to establish the criteria to determine where the radar should look to maintain the current track. When the radar identifies a target to track, it adjusts the tracking beam to examine the target from multiple beam angles. This improves the accuracy of the azimuth, elevation and range estimations of its true position. Using more than one beam to track a target necessarily means that, in a given amount of time, there are fewer beams that scan the rest of the field of view. A minimum optimal performance from the Kalman filter is needed to ensure the target(s) of interest are tracked accurately while still maintaining sufficient search time to locate potential new tracks.

Three other user-configurable parameters were adjusted from the defaults for this test. For each hemisphere dimeter, the minimum RCS mask parameter was set at a level to ensure the hemisphere radar signature would generate a track. The mask was used to eliminate any potential multipath backscatter returns from being tracked. A range mask was used to remove all target tracks occurring beyond the range of the Doppler rail system and the confidence level for each test was set conservatively at 15. The confidence level represents the radar's confidence from 0 for no confidence to 100 for maximum confidence that the data feeding the track comes from a real object and not from clutter or noise.

Doppler Target Measurements

Figure 6 presents track data measurements taken on a 12 in. hemisphere for state variance settings of 0.1, 0.2, 0.5 and 1.0. Figure 6(a) shows the radar cross section (RCS) in dBsm on the vertical axis and track time in seconds on the horizontal axis. The radar calculates an estimated RCS value based on the antenna gain, transmit power, receiver gain, IF filter transfer functions and A/D correction factors. The algorithm does not take into account the reduction in antenna gain at off normal field of view angles. A summary of the theoretical hemispherical value, the average RCS, and the RCS standard deviation for reach run is presented in Table 1.

Since the theoretical RCS value of the 12 in. hemisphere is known to be -11.4 dBsm, comparing it to the radar's estimated RCS value can help provide insight on the RCS masking levels that might be used in the radar algorithm to limit the number of targets being tracked during flight operations. For variance values from 0.1 to 0.5, the average RCS values lie between 2.19 and 2.68 dBsm with a standard deviation below 1. The average RCS for the variance of 1.0 data curve is 3.7 dB lower than the lowest of the other 3 variance values and the standard deviation is more than two times greater. The radar's estimated average RCS values for the 12 in. hemisphere are around 10 dB higher than the theoretical

value. Backscatter diffraction from the hemisphere edges in conjunction with potential multipath scatters occurring within the 3.25 m range bin could possibly account for a few dB variation in the instantaneous RCS value in these measurements.

Table 1. Summary of radar estimated RCS performance data.

Target Sphere Diameter, in	Variance	Theoretical RCS, dB	Average RCS, dB	Standard Deviation
12	0.1	-11.4	2.68	0.77
12	0.2	-11.4	2.19	0.86
12	0.5	-11.4	2.39	0.84
12	1	-11.4	-1.53	1.99
8	0.1	-14.9	-0.83	1.67
8	0.2	-14.9	-3.99	1.61
8	0.5	-14.9	-5.02	1.48
8	1	-14.9	-4.16	1.82
6	0.1	-17.4	-6.34	1.87
6	0.2	-17.4	-8.10	1.98
6	0.5	-17.4	-6.04	2.12
6	1	-17.4	-5.26	1.47
3	0.1	-23.4	-7.08	2.91
3	0.2	-23.4	-8.81	2.21
3	0.5	-23.4	-5.77	2.29
3	1	-23.4	-4.76	1.06

Figure 6 (b) thru (e) present range data for the 4 different variance values. The vertical axis is the straight line range distance to the moving hemisphere in meters and the horizontal axis is time in seconds. The Doppler rail target was measured with a laser distance finder to be approximately 22.5 meters at its closest point to the radar for the 12 in. hemispherical target. The Doppler target travel distance remained constant at 4.5 m for each hemispherical target, but the target's closest and furthest point to the radar shifted slightly based on the radius of the hemisphere and length of the attachment bolt securing it to the wood support. A background shading on the plot is provided to represent the full Doppler target travel distance of 4.5 m which accounts for the radar look down angle of about 26° at its furthest range. The data shows as the variance value is increased, the estimated range expanse of the 12 in. hemisphere Doppler target motion gradually improved. A variance setting of 0.5 maintained the best representation of the actual target position. A setting of 1.0 variance appeared to have the most inconsistent reported range of motion and frequently overestimated the actual position.

Figure 6(f) thru (i) presents the velocity of the 12 in. hemisphere in meters per second on the vertical axis and time in seconds on the horizontal axis. The Doppler target is programmed to accelerate for 0.35 sec before it reaches a constant velocity of 2.33 m/s for 1.83 sec. The target then decelerates for 0.35 sec before immediately reversing direction. The gray background shading indicates the expected constant velocity of the Doppler target at ±2.3 m/s for variance values below 0.2, the velocity is underestimated by a little more than 1.0 m/s. At 0.5 variance the velocity is typically underestimated by 0.3 m/s. For the variance setting at 1.0, the correct velocity of 2.3 m/s is occasionally reported. The greater the variance, the faster a change in target velocity will be reported in the track velocity output. However, increasing the variance also causes the track velocity estimate to become noisier which can be easily observed in Figure 6(i).

Figure 7 presents track data measurements taken on the 8 in. hemisphere for variance settings of 0.1, 0.2, 0.5 and 1.0. Figure 7(a) presents the RCS value in dBsm on the vertical axis and time in seconds on the horizontal axis. The theoretical RCS value for an 8 in. hemisphere is -14.89 dBsm. The average RCS values for the variance settings of 0.1, 0.2, 0.5 and 1.0 were calculated to be -0.83, -3.99, -5.02 and -4.16 dBsm respectively (see Table 1). The radar's average reported RCS value is 9.87 dB higher than the theoretical value at 0.5 variance and 14 dB higher at 0.1 variance. The standard deviation varied from 1.48 for the 0.5 variance measurement out to 1.82 for a variance of 1.0. The RCS value looks to be considerably more constant for the variance of 0.1 out to 90 sec, but then the value drops 7 dB causing the standard deviation to 1.67.

Figure 7(b) thru (e) present range data for the 4 different variance values. The vertical axis is the range distance in meters and the horizontal axis is time in seconds. The data trend generally shows as the variance value is increased, the estimated range expanse of the hemisphere Doppler target also generally increases. The 8 in. hemisphere range data for 0.1 variance looks comparable to the 12 in. hemisphere data shown in Figure 6(b). At the other variance settings, the 8 in. hemisphere range data appears to be noisier and less consistent in matching the known track position.

Figure 7(f) thru (i) presents the velocity of the 8 in. hemisphere in meters per second on the vertical axis and time in seconds on the horizontal axis. For variance value of 0.1, the velocity is generally underestimated by

about 1.3 m/s. For the variance setting at 1.0, the correct velocity of 2.3 m/s is often correctly reported. The track velocity estimate does again become noisier with increasing variance settings, but overall provides a more accurate velocity representation even with the noise.

Figure 8 presents track data measurements collected using the 6 in. hemisphere as the Doppler target for the same four variance settings as before. Figure 8(a) presents the RCS value in dBsm on the vertical axis and time in seconds on the horizontal axis. The theoretical RCS value for a 6 in hemisphere is -17.4 dBsm. The average RCS values for the variance settings of 0.1, 0.2, 0.5 and 1.0 were calculated to be -6.34, -8.1, -6.04 and -5.26 dBsm respectively. The radar's average reported RCS value is about 12 dB higher than the theoretical value at a variance setting of 1.0 and 9.3 dB higher in the closest comparison at 0.2 variance. The standard deviation varied from 2.12 for the 0.5 variance measurement down to 1.47 for a variance of 1.0. This is a reversal from the 8 inch data which showed the least standard deviation at 0.5 variance and the largest deviation at 1.0 variance.

Figure 8(b) thru (e) presents the range data for the 4 different variance settings. The vertical axis is the range distance in meters and the horizontal axis is time in seconds. The data trend once again generally shows as the variance value is increased, the estimated range expanse of the hemisphere Doppler target also generally increases. The 6 in. hemisphere range data for 0.1 variance has degraded considerably comparable to the 12 in. and 8 in. hemisphere data shown in Figure 6(b) and 7(b) respectively. At the other variance settings, the 6 in. hemisphere range data approximated the corresponding 8 in. hemisphere measurement in the characteristics of the noise and position inaccuracies.

Figure 8(f) thru (i) presents the velocity data of the 6 in. hemisphere in meters per second on the vertical axis and time in seconds on the horizontal axis. The reported velocity profile in Figure 8(f) does not show the same square wave pattern as the 8 in. hemisphere in Figure 7(f) or the 12 in. hemisphere in Figure 6(f) for variance settings of 0.1. For the variance setting at 1.0, the correct velocity of 2.3 m/s is once again often correctly reported, but also shows numerous occurrences where the velocity is a little higher than the 2.3 m target speed. The track velocity once again appears to be noisier with increasing variance.

Figure 9 presents track data measurements collected using the 3 in. hemisphere as the Doppler target for the same four variance settings. Figure 9(a) presents the RCS value in dBsm on the vertical axis and time in seconds on the horizontal axis. The theoretical RCS value for a 3 in. hemisphere is -23.4 dBsm. The average RCS values for the variance settings of 0.1, 0.2, 0.5 and 1.0 were calculated to be -7.08, -8.81, -5.77 and -4.76 dBsm respectively. The radar's average reported RCS value is about 18.6 dB higher than the theoretical value at a variance setting of 1 and about 14.6 dB higher in the closest comparison at 0.2 variance. The standard deviation varied from 2.91 in the worst case for the 0.1 variance measurement down to 1.06 for a variance of 1.0 in the best case. The standard deviation at a given variance setting steadily grew as the size of hemisphere reduced in size except when the variance was set to 1.0. In this case the trend reversed and the standard deviation actually improved with decreasing the size of the hemisphere.

Figure 9(b) thru (e) presents the range data for the 4 different variance settings. The vertical axis is the range distance in meters and the horizontal axis is time in seconds. The data trend once again generally shows as the variance value is increased, the estimated range expanse of the hemisphere Doppler target also generally increases. The 3 in. hemisphere range data for 0.1 variance is still degraded over the comparable 12 in. and 8 in. hemisphere data shown in Figure 6(b) and 7(b) respectively. The 0.5 and 1.0 variance setting data look considerably less noisy than the prior 6 in. hemisphere range data presented in Figure 8(d) and (e). The range profile for the 3 in. hemisphere at a variance of 1.0 looks as good as the corresponding 12 in. hemisphere range data. This is somewhat surprising since the actual signal to noise ratio should have decreased by 12 dB based on the RCS of the 3 in. and 12 in. diameter hemispherical Doppler targets.

Figure 9(f) thru (i) presents the velocity data of the 3 in. hemisphere in meters per second on the vertical axis and time in seconds on the horizontal axis. The velocity profile in Figure 9(i) for the variance setting at 1.0 correctly reports the velocity at 2.3 m/s pretty reliably with less numerous overshoots as observed in other sized hemisphere data. No significant increase in the noise level is observed in relation to increasing the variance on the 3 in. hemisphere as was noted for the 6

in. hemisphere data.

Radar Antenna Measurements

The Metamaterial Electronically Scanning Array (MESA) antenna was measured to determine its relative gain, and side lobe levels and half power beam width (HPBW) at boresight compared to extreme field of view pointing vectors. The gain of the antenna directly relates to the radar's detection range and a significant drop in gain over the radar field of view would limit the radar's ability to detect air traffic at those viewing angles. The MESA antenna can be held at any pointing vector within the ±60° azimuth and ±40° elevation field of view. New experimental methods were developed to achieve this assessment since proprietary restrictions on accessing the radar antennas. This prevented standard practice antenna measurements which incorporate a network analyzer to both transmit and receive the radiated signal. A spectrum analyzer was integrated with the ETR data acquisition system to receive the radar's transmission to conduct the measurements. The radar was mounted on a rotational tilt stage in the center of the ETR quite zone and data was collected at 1° azimuthal increments. The radar MESA antenna was configured to transmit at a constant azimuth and elevation position for each measurement. The radiation was measured at the ETR feed location using a K-band antenna connected to the spectrum analyzer set on max hold. The general setup between the radar and the receive antenna is sketched in Figure 10. To keep the center of the transmitted beam pointed at the vertical center of the ETR reflector, the tilt stage was elevated downward at the corresponding angle the MESA beam was pointing up in elevation. The tilt stage can be elevated in 10° increments and was set to either 0°, 30°, or 40° elevation angles for these tests. With the MESA antenna beam held at a constant pointing vector, the radar was then physically rotated in one degree increments to acquire the radiation pattern.

The antenna patterns were first measured without the radar being installed on a UAS. Four separate antenna measurements were conducted to examine the H plane radiation pattern at different MESA pointing vectors and two E plane measurements. The H plane measurement required the radar to be installed on the azimuth stage rotated 90° on its side to transmit in vertical polarization. The radar would normally be operated to transmit with the electric field horizontal to the earth. Rotating the radar 90° and the receive antenna rotated to vertical polarization allowed the H plane pattern to be collected. Figures 11 and 12 show the E plane and H plane setup along with angle definitions. The MESA antenna beam was set to point at 0° azimuth and 0° elevation for the first measurement. Figures 13 (a) shows the H plane radiation pattern for the MESA beam pointing at 0° azimuth, 0° elevation. The x axis is the rotation angle of the radar in degrees. The y axis is the received power in dBm. The peak power is -24 dBm and the maximum side lobe level is 18 dB below the peak. The half power beam width is shown to be about 12°. The beam width and side lobe levels appear to be at acceptable levels to meet airborne tracking operations. For the next three H plane measurements, the MESA azimuth angle remained at 0°, while the elevation was changed to -20°, -40° and +40°. Figures 13 (b), (c), and (d) presents the H plane radiation pattern for the MESA beam pointing at 0° azimuth, and -20°, -40° and +40° elevations respectively. The peak power was -24.4 dBm at -20° elevation, -26.6 dBm at -40° elevation and -25.4 at +40° elevation. For the 0° azimuth, -40° elevation beam angle the relative gain has dropped by 2.6 dB in transmitted peak power. This equates to a 5.2 dB reduction in received power for radar operations which would reduce detection range by 26% at the extreme field of view angles. The maximum side lobe levels were 14.9, 13.4 and 13.9 dB below the peak respectively. The half power beam width became broader at the extreme elevation angles. At -40° elevation the HPBW was about 21° and about 19° at +40° elevation, expanding from 12° nominal at boresight.

The E plane radiation patterns (shown in Figure 14) were conducted by rotating both the radar and the receive antenna to Horizontal polarization. Figure 14(a) shows the E plane antenna pattern for the MESA antenna pointing to 0° azimuth and 0° elevation. The peak power is -24.3 dBm and the maximum side lobe level is 15.7 dB below the peak. The half power beam width is shown to be about 5°. Figure 14(b) presents the E plane radiation pattern for the MESA pointed at 0° azimuth and +40° elevation. The peak power is about -26 dBm with a HPBW of 6°. The maximum side lobe level is about 24 dB down from the peak.

The radar was then installed on a candidate sUAS

(shown in Figure 15) to evaluate the E plane radiation pattern and verify that the radar's operational field of view was not impacted due to the static rotor motor and propeller line of sight blockage. Figure 16(a) shows the E plane radiation pattern with the radar installed on the UAS for the MESA pointing at 0° azimuth and +40° elevation. The peak power is -26 dBm, the same value as in Figure 14(b). The maximum side lobe level and HPBW are also not impacted by the UAS installation. Figure 16(b) (run 6) presents the E plane radiation pattern for the MESA pointing at 0° azimuth and 30° elevation. The main beam peak power is -25.6 dBm. The maximum side lobe level is 20 dB below the peak. The HPBW is about 5.5°. The MESA beam was then measured at 30° azimuth and 30° elevation and is shown in Figure 16(c). The radiation pattern looks similar to the 0° azimuth beam and does not appear to be influenced by the sUAS. To ensure the MESA beam was pointed in an azimuth direction in line with one of the motors, a test was conducted with the beam pointing at 22° azimuth and 30° elevation as shown in Figure 16(d). The gain, HPBW and side lobe levels do not appear to be impacted by the sUAS static motor and blades. The final measurements were conducted at 40° elevation at azimuth angles of 20°, 22°, 24° and 26° degrees azimuth. These measurements are combined in one plot shown in Figure 17 for comparison. No apparent beam degradation is observed in the data curves. The radar installation on the candidate sUAS does not appear to have degraded the antenna beam performance for the field of view angles observed. Future sUAS radar measurements will incorporate a 6 axis robotic arm to provide higher elevation angle measurement fidelity and simplify the measurement process.

Summary

Indoor ground tests were performed on a candidate commercially available sense and avoid 24.5 GHz Doppler radar for the NASA UTM project prior to being flown outdoors to evaluate the radar's capabilities to locate, track and alert the presence of airborne vehicles for the purpose of autonomous maneuvering. The tests were conducted inside the NASA Langley Research Center's Experimental Test Range (ETR) from a stationary platform to evaluate the Doppler radar performance characteristics and also develop operational proficiency using the radar before the SAA sensor was allowed to be operated outdoors.

A high speed linear rail actuator system was developed to generate Doppler targets. Four different sized copper hemispheres were tested independently on the linear rail to generate Doppler targets of varying radar signatures. The tests were repeated with changes to the state variance parameters to evaluate the response from the Kalman filter. Tracking data was plotted to show the Doppler targets estimated RCS, range and velocity. The linear rail system developed provided an effective method to generate Doppler targets of known RCS for indoor radar evaluations.

Measurement comparisons between the radar's recorded track data's average estimated radar cross section values from the various sized hemispheres with the hemisphere's known specular reflection showed the reported RCS was 9.3 dB higher in the best comparison. This discrepancy is reported to be associated largely with the internal high pass filter transfer function, and is expected to be improved in a future firmware update.

The accuracy of the radar's range estimate to the Doppler target was shown to be influenced by changes in the variance setting. For the 12 in. hemisphere tests, the low variance settings caused the Kalman filter to consistently underestimate the actual position of the Doppler target. Increasing the variance to 0.5 provided a good estimate of the reported range position. However, for other sized hemispheres, the range data appeared noisy in several data plots and no clear trend stood out. The noise in the range data was not solely correlated to the signal to noise level of the Doppler target, but it is believed to be an influencing factor.

The accuracy of the velocity estimate was also shown to be very sensitive to changes in the variance value. A low variance setting of 0.1 caused the Kalman filter to under estimate the true velocity by as much as 1 m/s. A variance setting of 1.0 provided the most accurate speed estimate, but also sometimes overestimated the true speed. Several of the velocity data plots also appeared noisy and prevented good trends to be developed across the entire data set.

Antenna measurements were performed with the radar installed both on and off a sUAS to quantify the relative antenna gain, beam width, and side lobe levels of the

radar's Metamaterial Electronically Scanning Array (MESA) when pointed at boresight and extreme field of view pointing vectors. The relative gain of the antenna was measured to be 2.6 dB lower in transmitted power at -40° elevation compared to 0° elevation at 0° azimuth. This equates to a 5.2 dB reduction in received power for radar operations and is a reduction in range detection by 26% at the extreme angles. For targets being observed between + 20° and - 20° elevation angles, the gain reduction is typically less than 1.5dB, resulting in less than 3dB two-way loss and less than 16% range reduction. Antenna measurements with the radar installed on a sUAS did not show signs of degradation due to line of sight blockage at the look angles tested. Future antenna testing in ETR will incorporate a 6-axis robotic arm to improve the fidelity of the positioning system.

The indoor radar evaluation was successful at developing an understanding of the radar operation and in integrating the tracking data with the NASA developed SAA algorithm ICAROUS. Outdoor flight testing of the radar with ICAROUS will be needed to thoroughly evaluate the radar's capabilities at achieving UTM objectives.

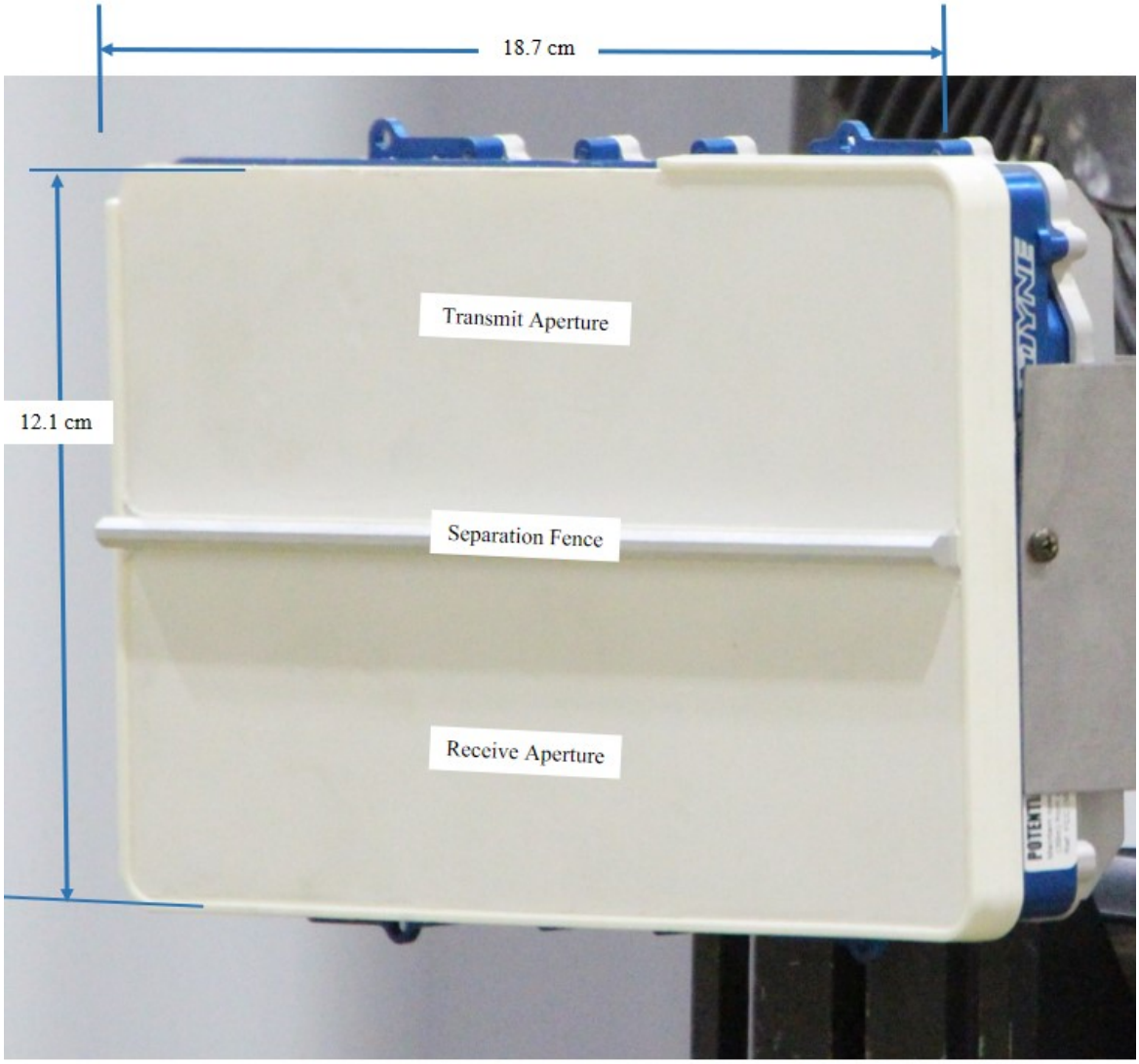

Figure 1. Photograph of radar mounted in ETR.

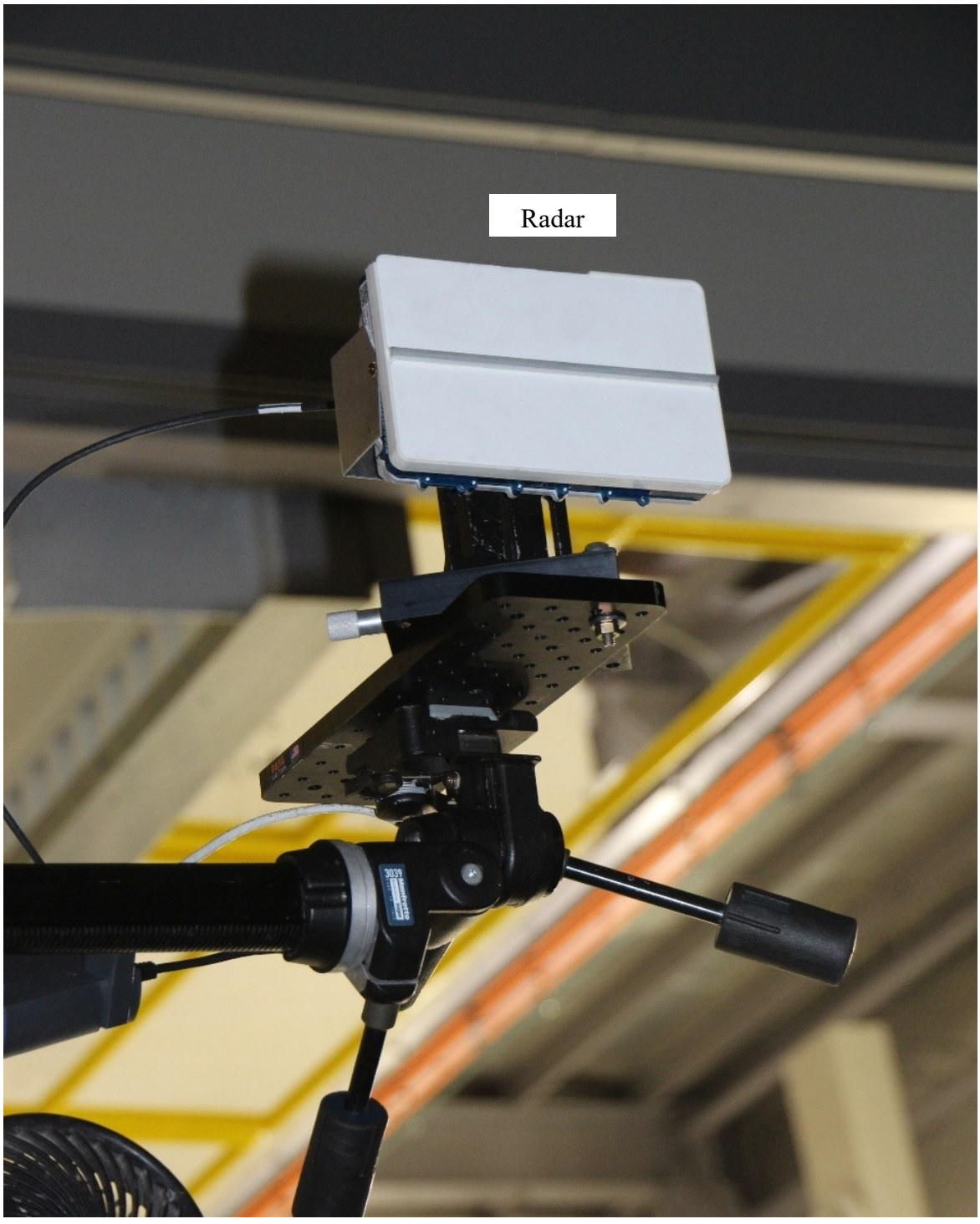

Figure 2. Photograph of radar mounted on tripod.

(a) View looking uprange in ETR toward the primary reflector.
Figure 3. ETR and setup configuration of indoor motion detect and track tests.

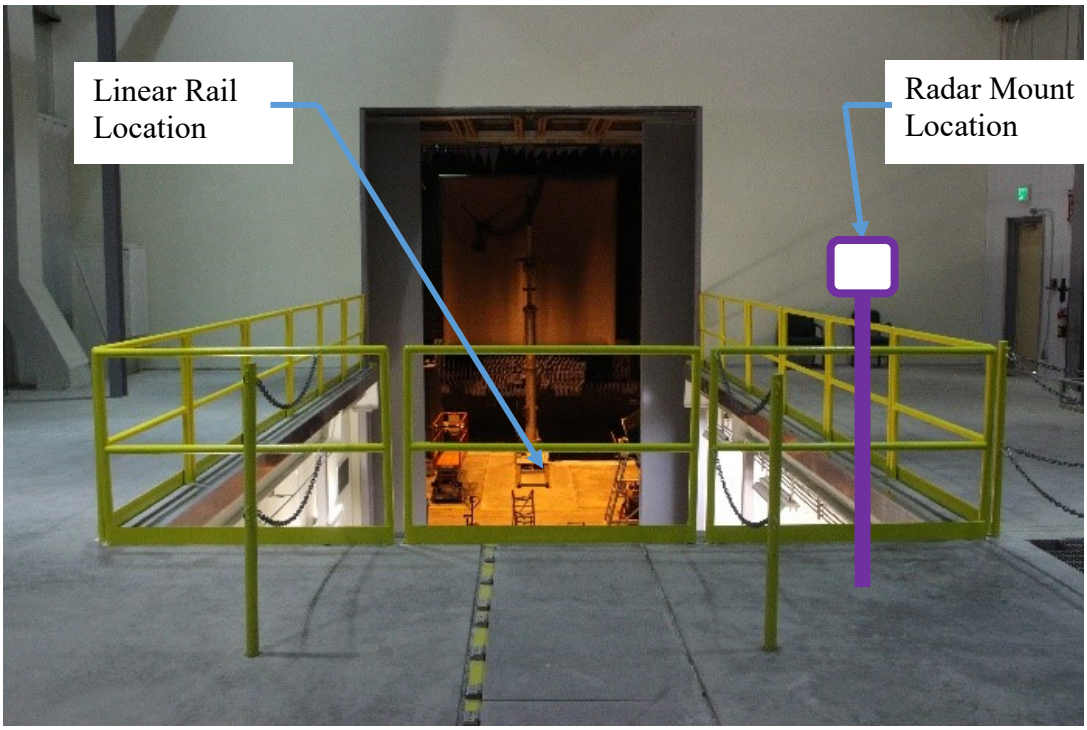

(b) View from mezzanine of radar stationary location toward linear rail location (see Figure 3(c) and (d)).
Figure 3. Continued.

(c) View from radar of indoor test setup toward linear rail.
Figure 3. Continued.

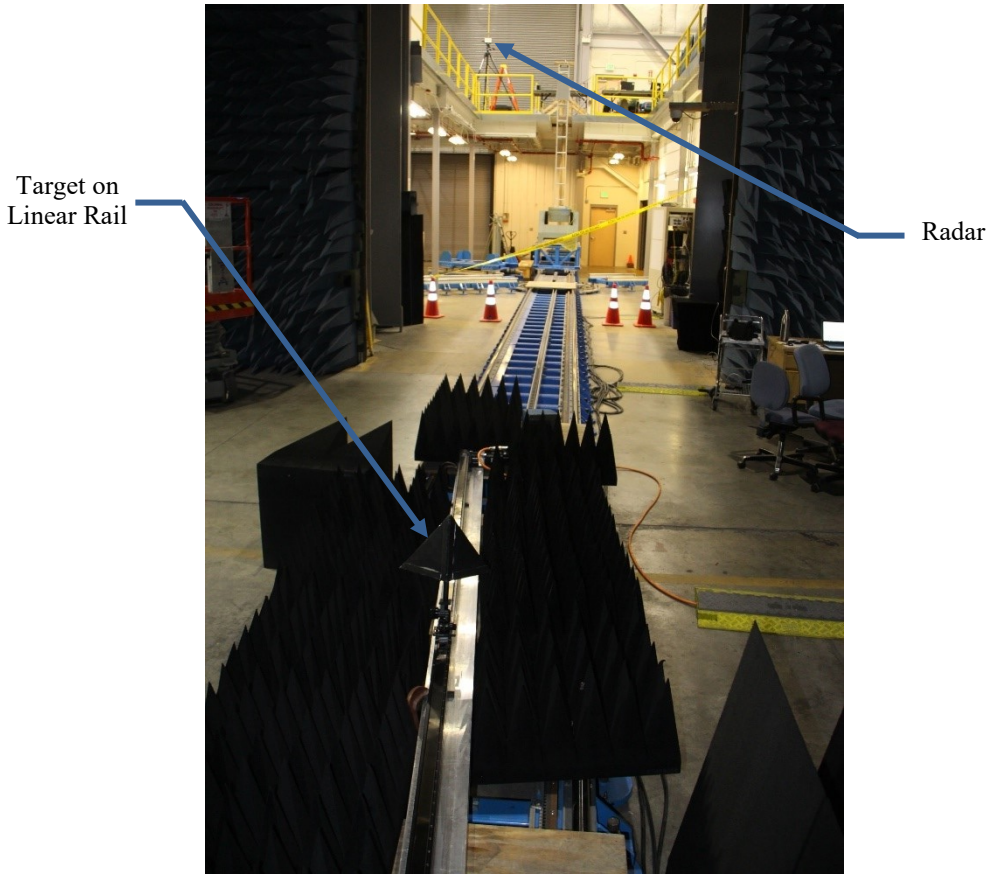

(d) View from linear rail assembly of indoor test setup.
Figure 3. Concluded.

Figure 4. Various sized hemispherical targets.

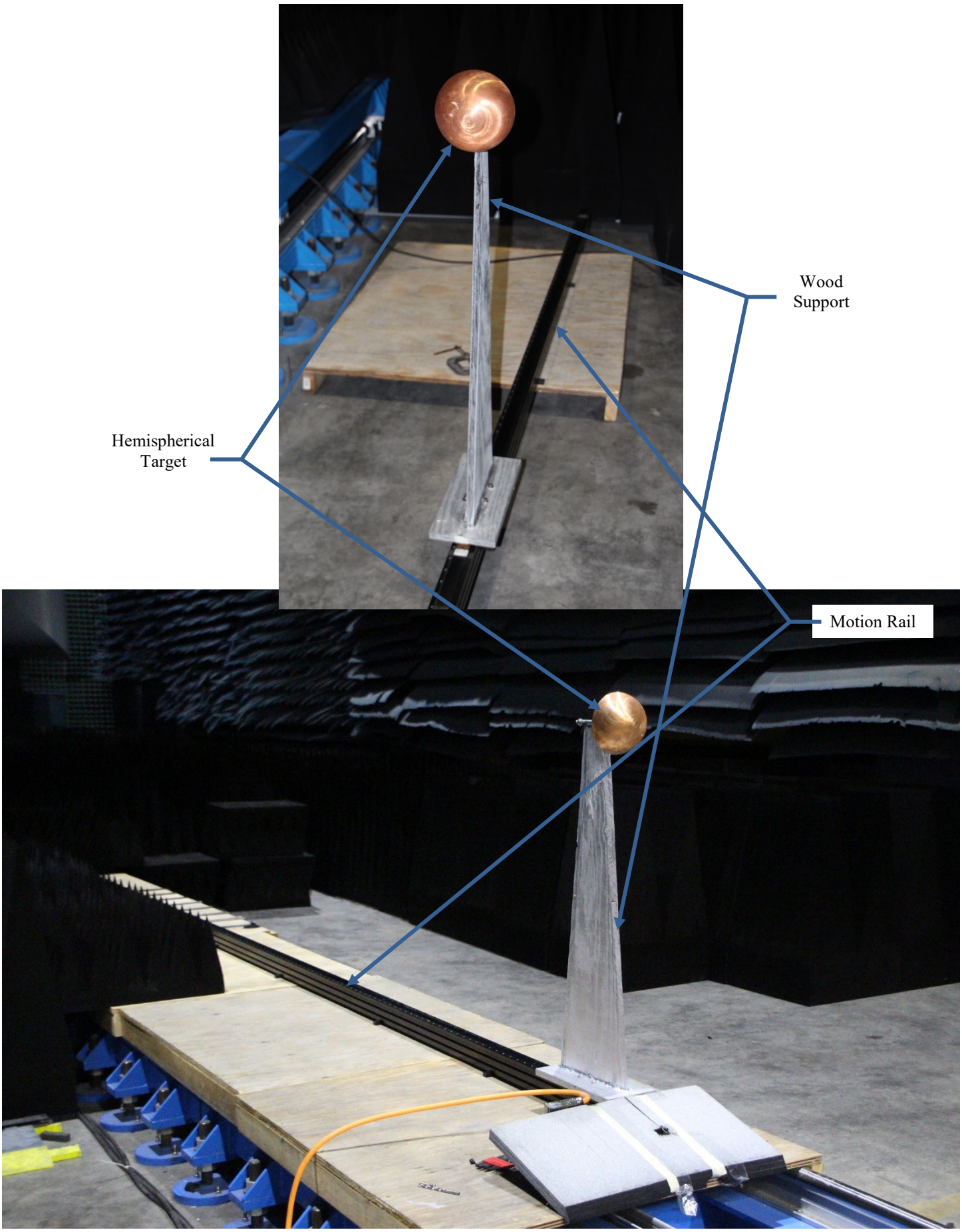

Figure 5. Hemispherical target mounted on wood support on 5 m long motion rail.

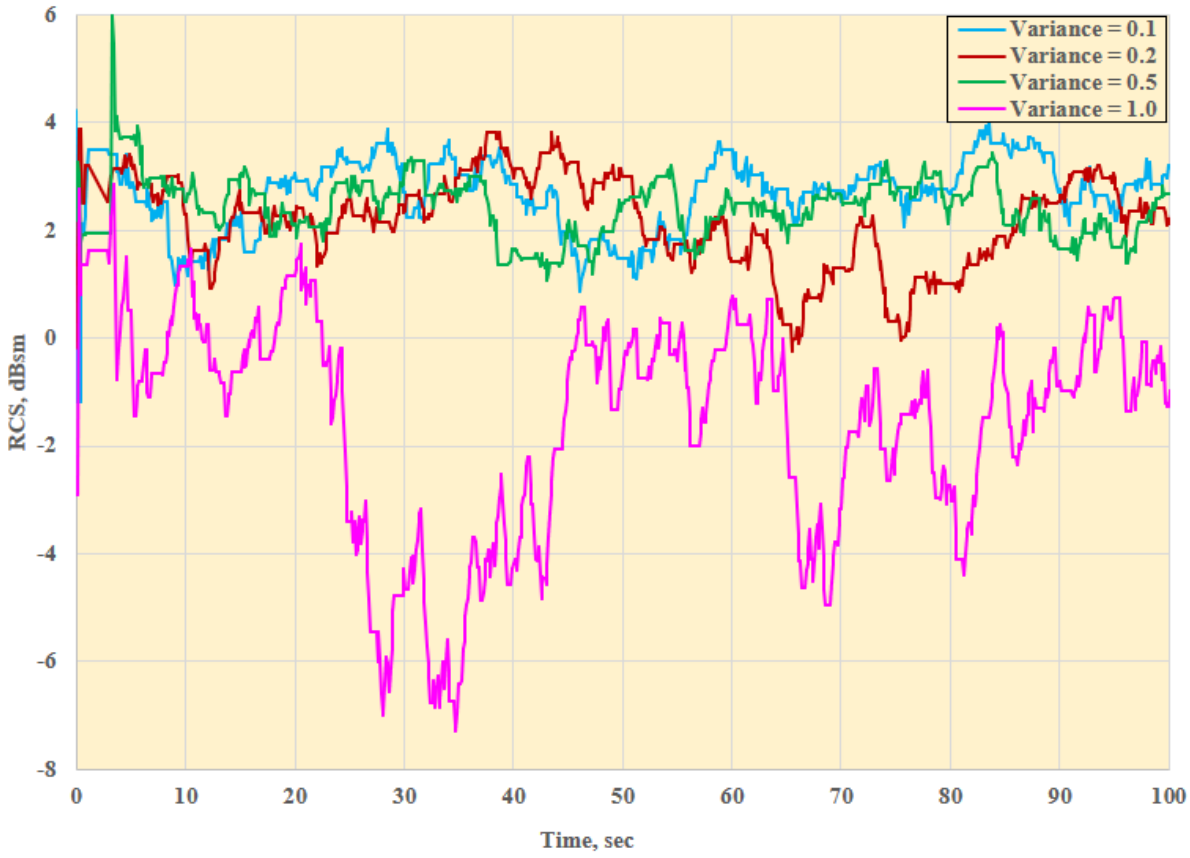

(a) RCS versus time using a 12 in. hemisphere.

Figure 6. Track data measurements for a 12 in. hemisphere with variance settings of 0.1, 0.2, 0.5, and 1.0.

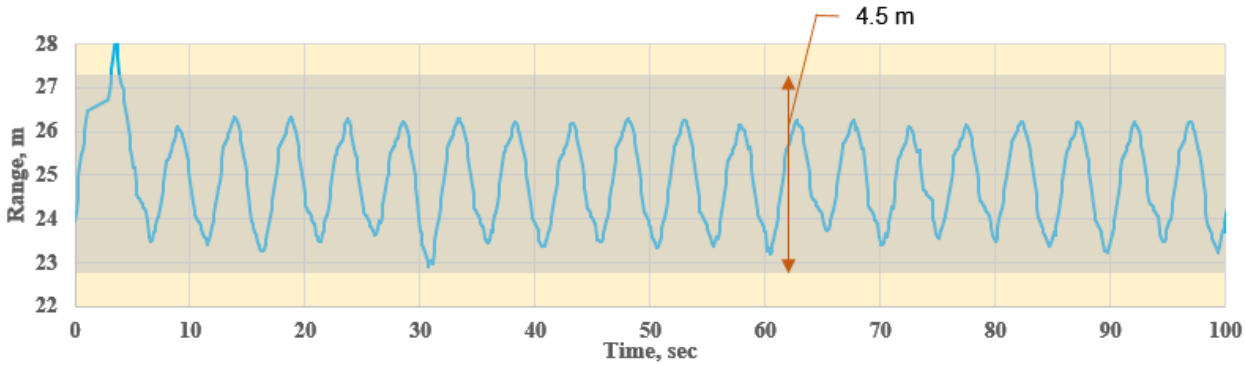

(b) Range versus time using a 12 in. hemisphere and variance = 0.1.
Figure 6. Continued.

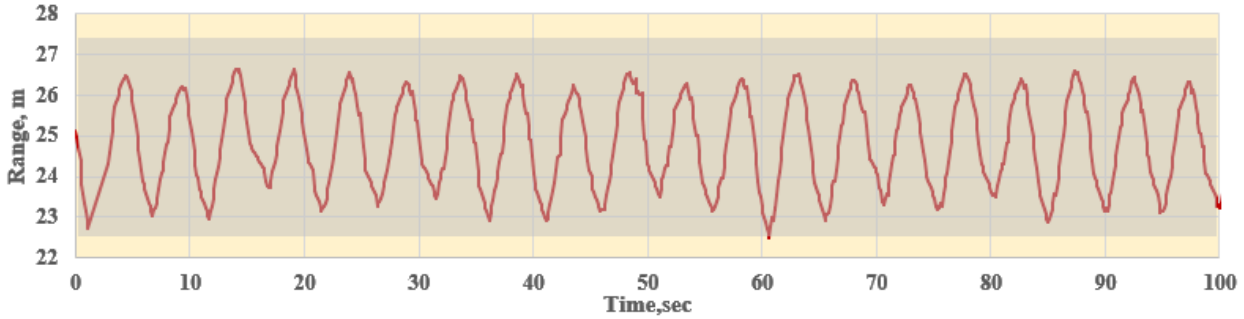

(c) Range versus time using a 12 in. hemisphere and variance = 0.2.
Figure 6. Continued.

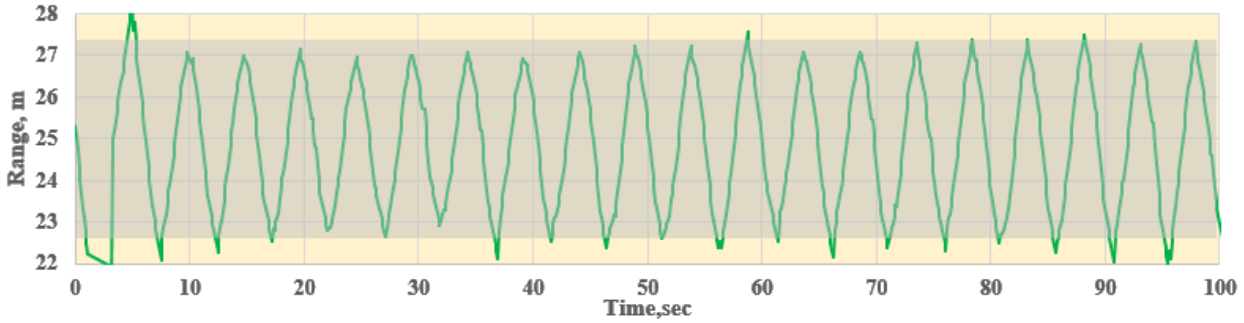

(d) Range versus time using a 12 in. hemisphere and variance = 0.5.
Figure 6. Continued.

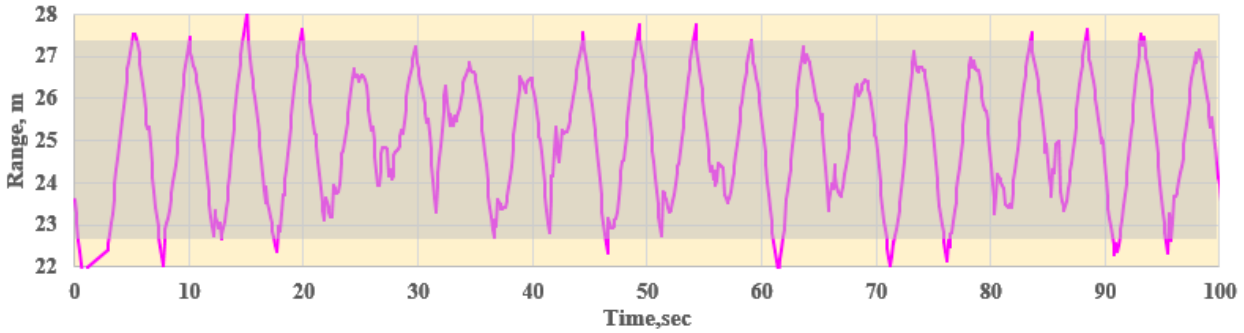

(e) Range versus time using a 12 in. hemisphere and variance = 1.0.
Figure 6. Continued.

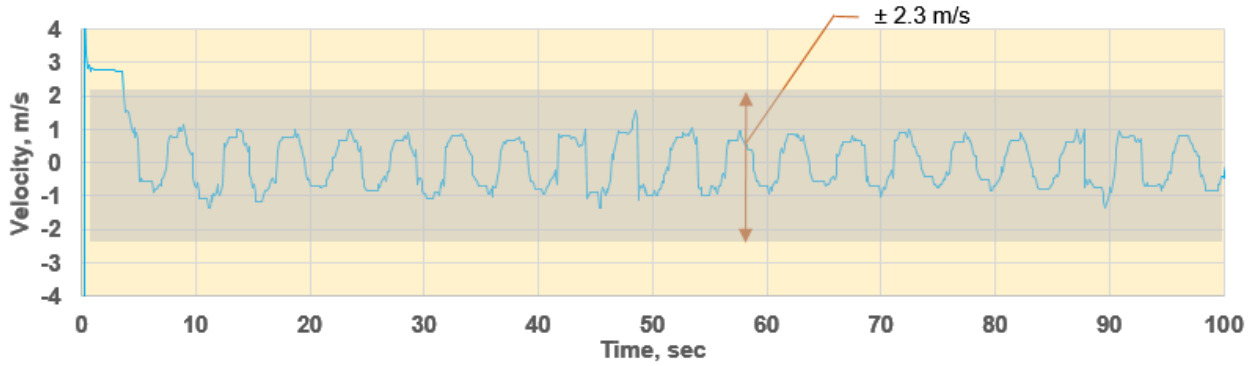

(f) Velocity versus time using a 12 in. hemisphere and variance = 0.1.
Figure 6. Continued.

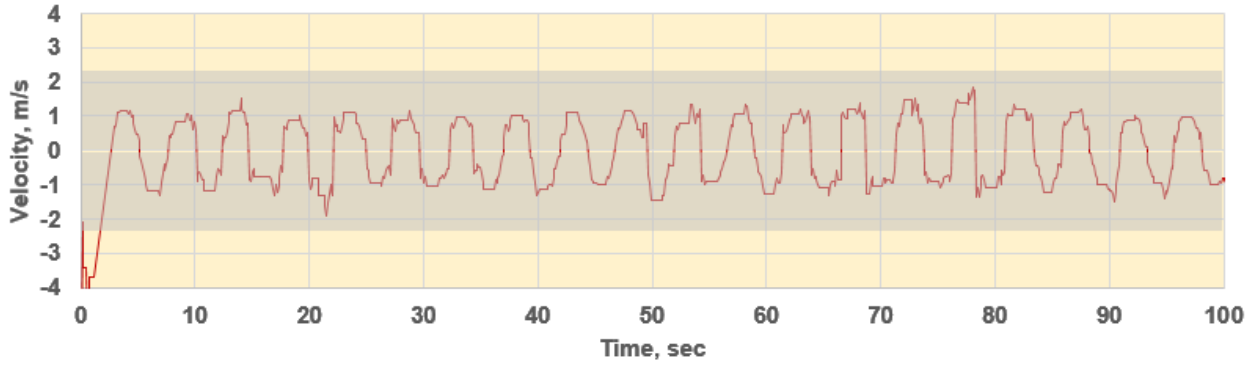

(g) Velocity versus time using a 12 in. hemisphere and variance = 0.2.
Figure 6. Continued.

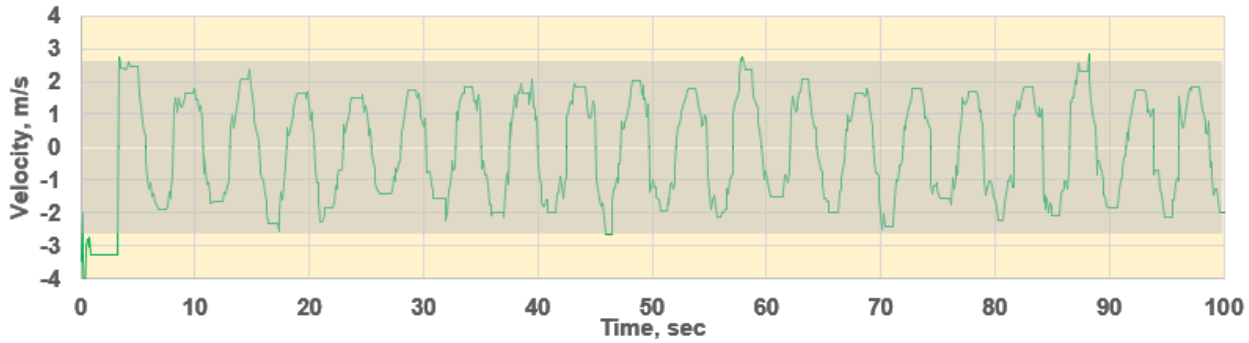

(h) Velocity versus time using a 12 in. hemisphere and variance = 0.5.
Figure 6. Continued.

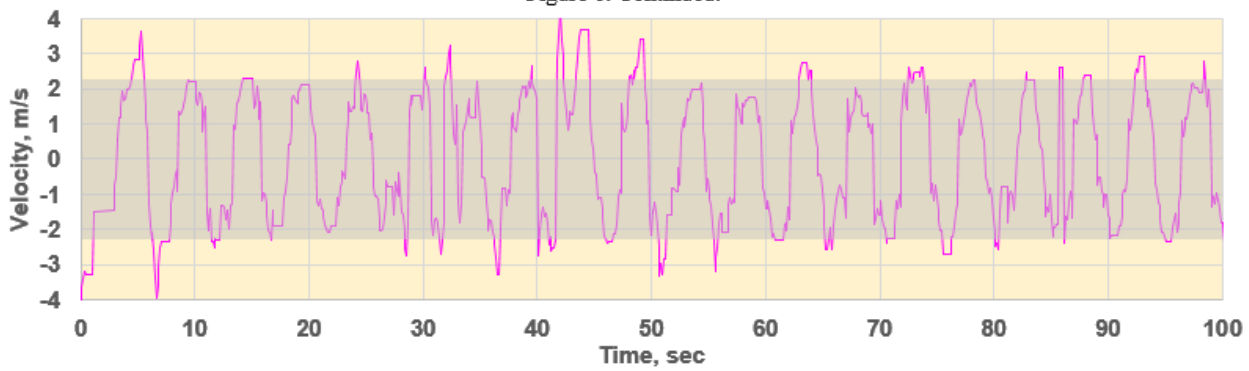

(i) Velocity versus time using a 12 in. hemisphere and variance = 1.0.
Figure 6. Concluded.

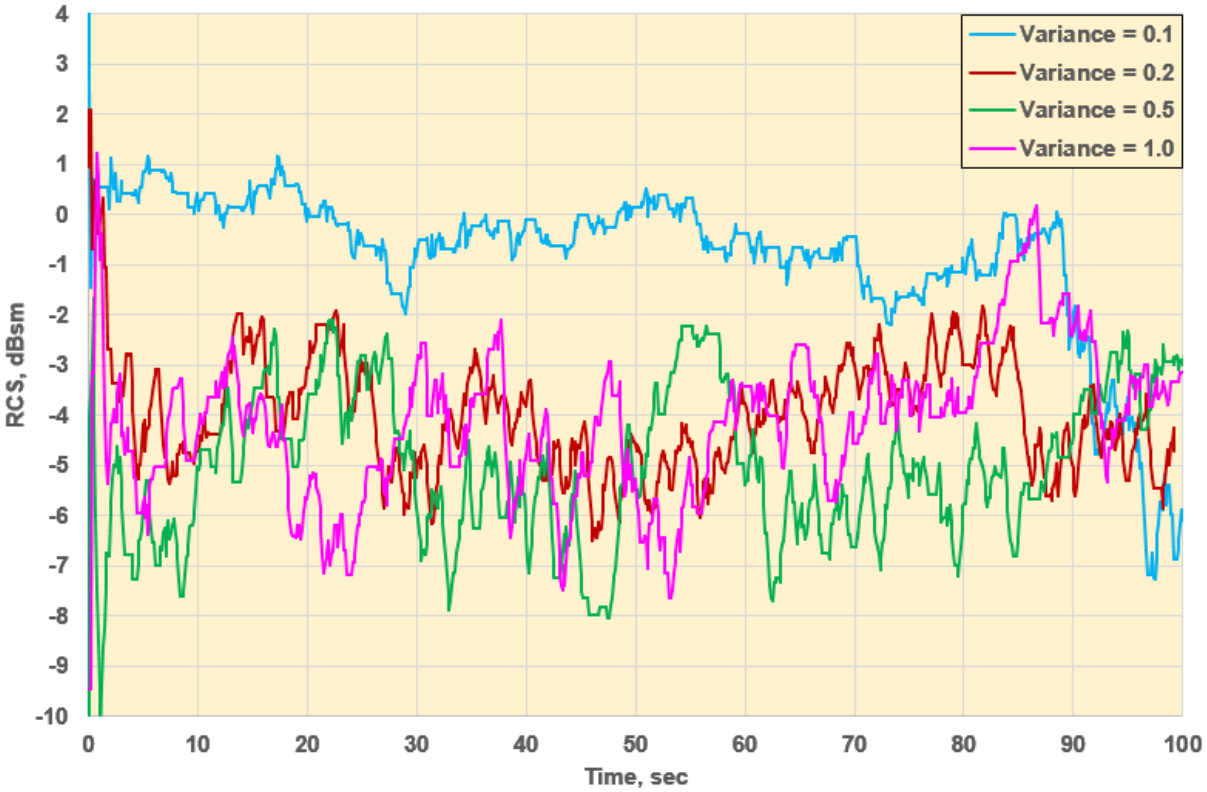

(a) RCS versus time using a 8 in. hemisphere.

Figure 7. Track data measurements for a 8 in. hemisphere with variance settings of 0.1, 0.2, 0.5, and 1.0.

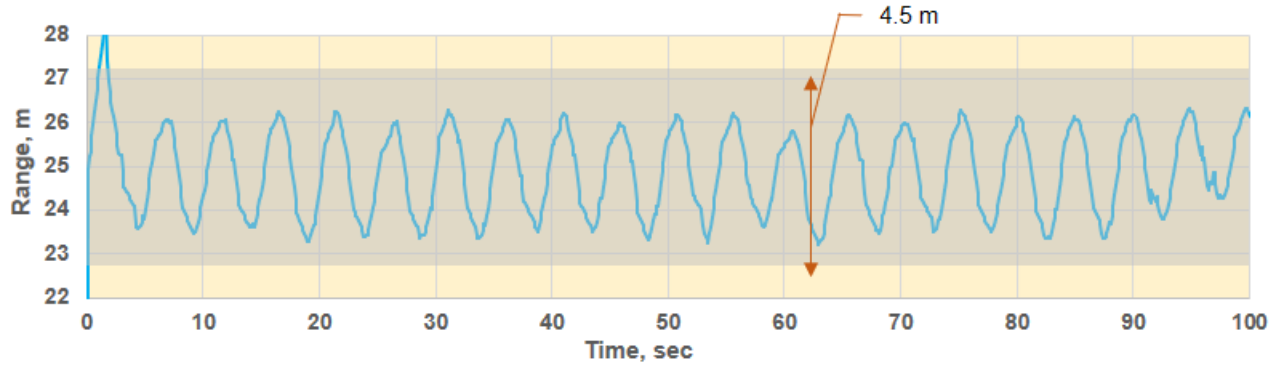

(b) Range versus time using a 8 in. hemisphere and variance = 0.1.
Figure 7. Continued.

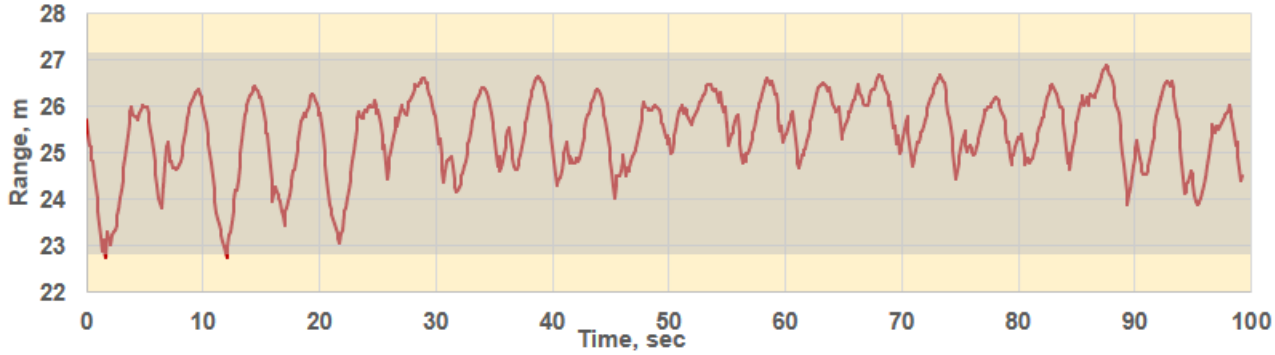

(c) Range versus time using a 8 in. hemisphere and variance = 0.2.
Figure 7. Continued.

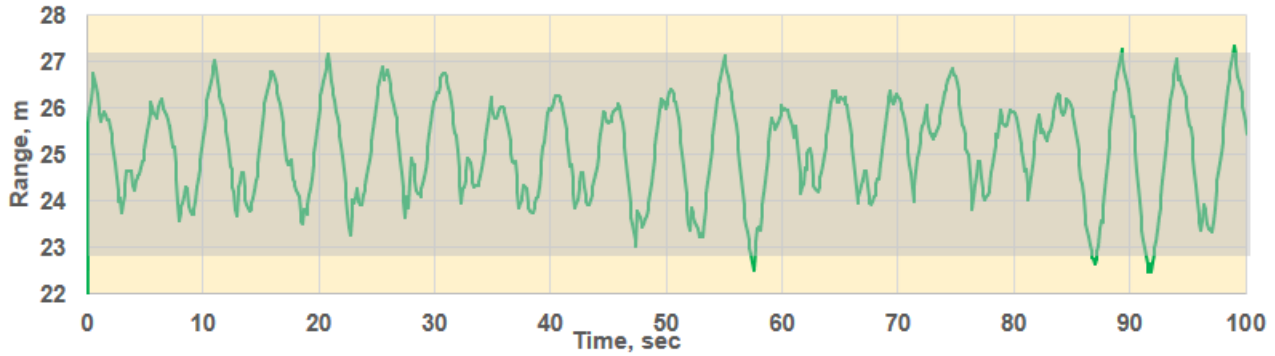

(d) Range versus time using a 8 in. hemisphere and variance = 0.5.
Figure 7. Continued.

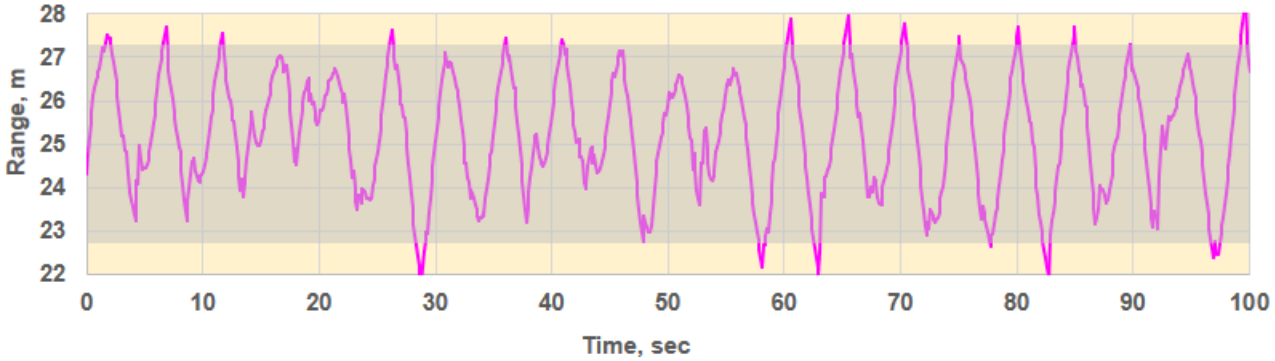

(e) Range versus time using a 8 in. hemisphere and variance = 1.0.
Figure 7. Continued.

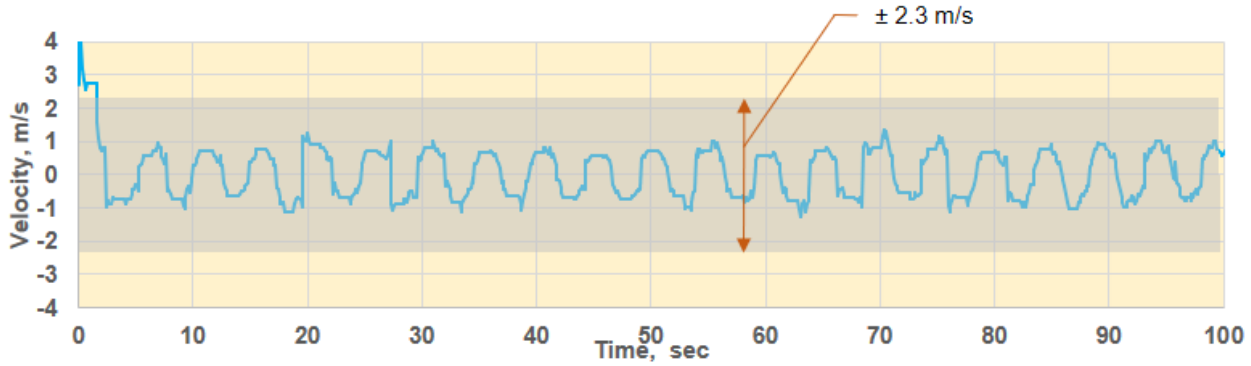

(f) Velocity versus time using a 8 in. hemisphere and variance = 0.1.
Figure 7. Continued.

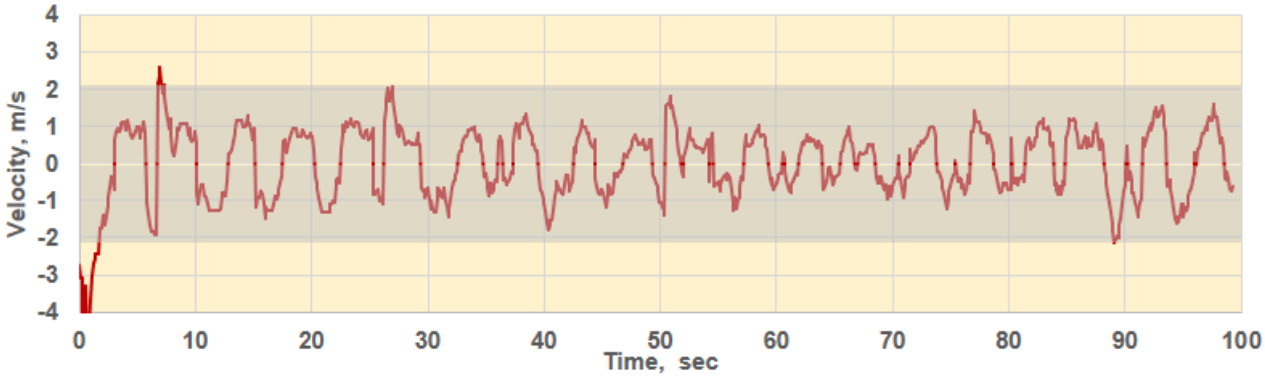

(g) Velocity versus time using a 8 in. hemisphere and variance = 0.2.
Figure 7. Continued.

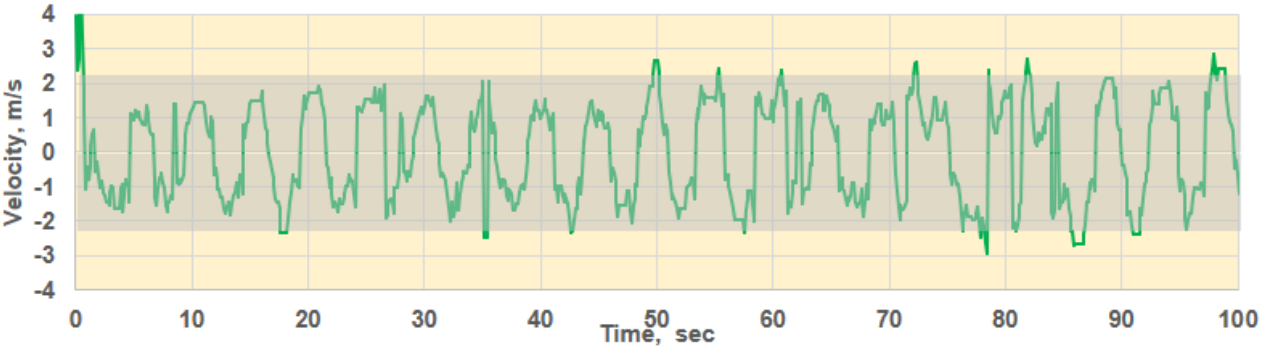

(h) Velocity versus time using a 8 in. hemisphere and variance = 0.5.
Figure 7. Continued.

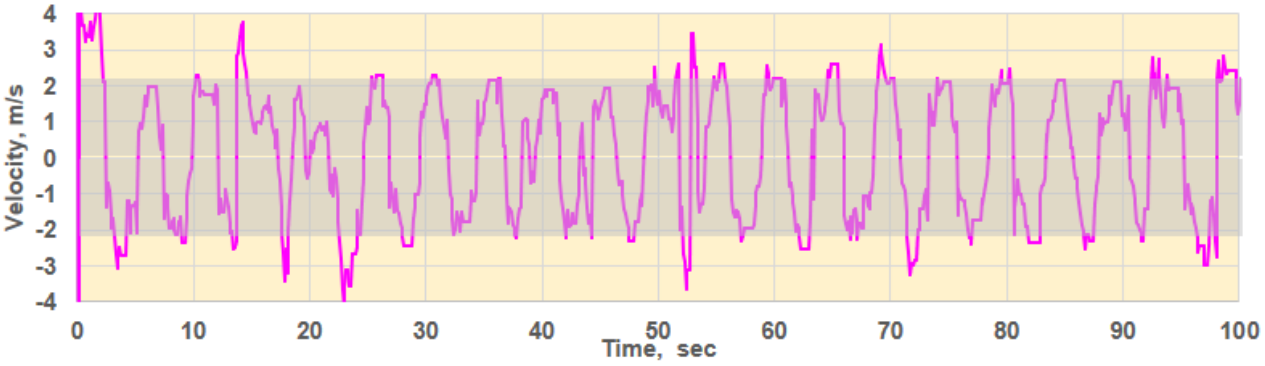

(i) Velocity versus time using a 8 in. hemisphere and variance = 1.0.
Figure 7. Concluded.

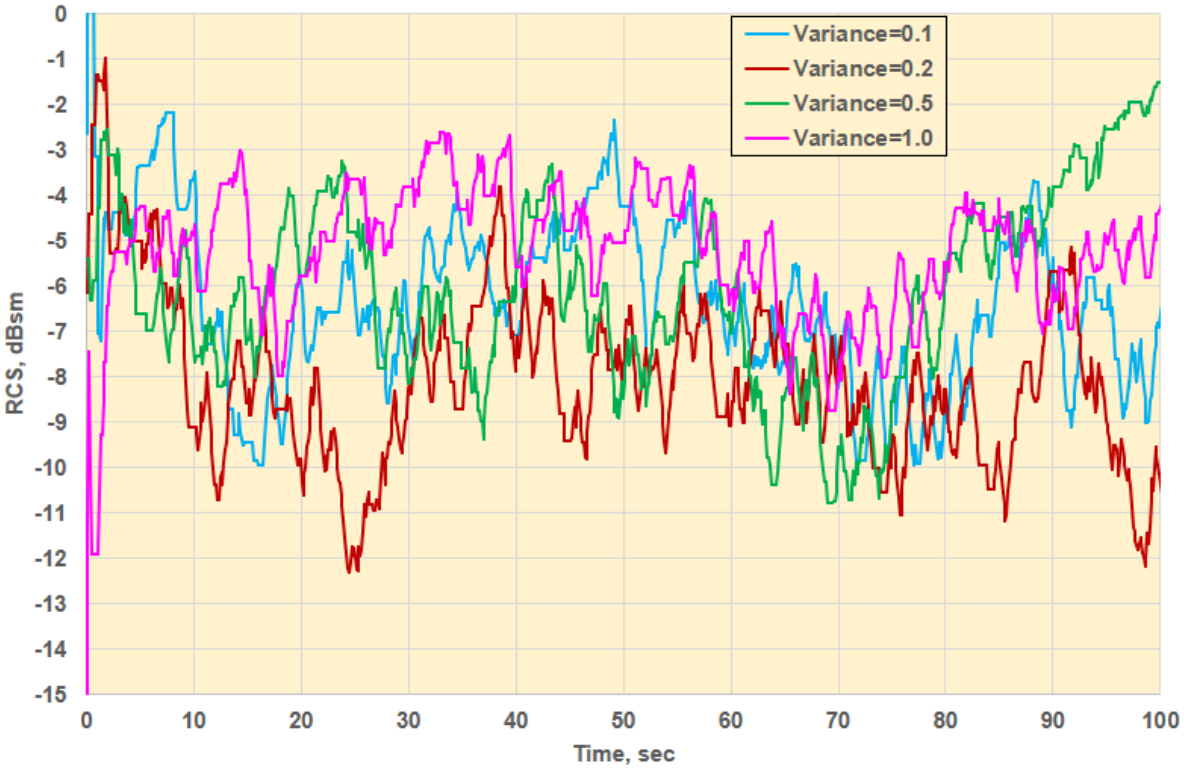

(a) RCS versus time using a 6 in. hemisphere.

Figure 8. Track data measurements for a 6 in. hemisphere with variance settings of 0.1, 0.2, 0.5, and 1.0.

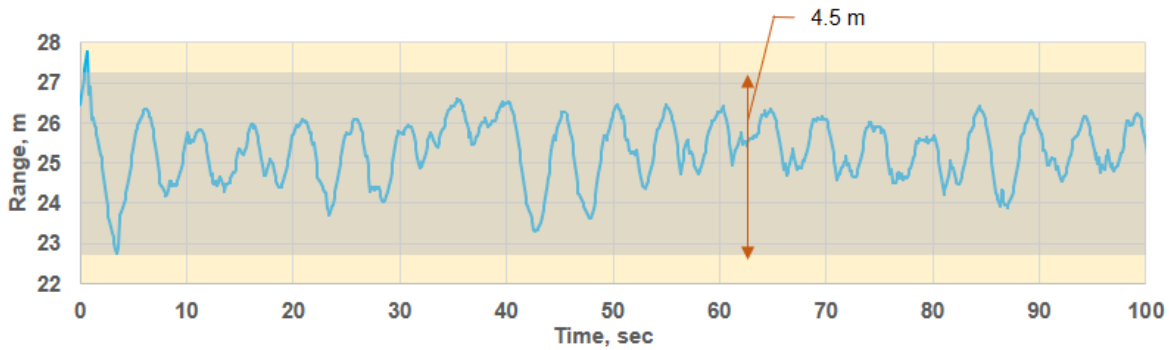

(b) Range versus time using a 6 in. hemisphere and Variance = 0.1.
Figure 8. Continued.

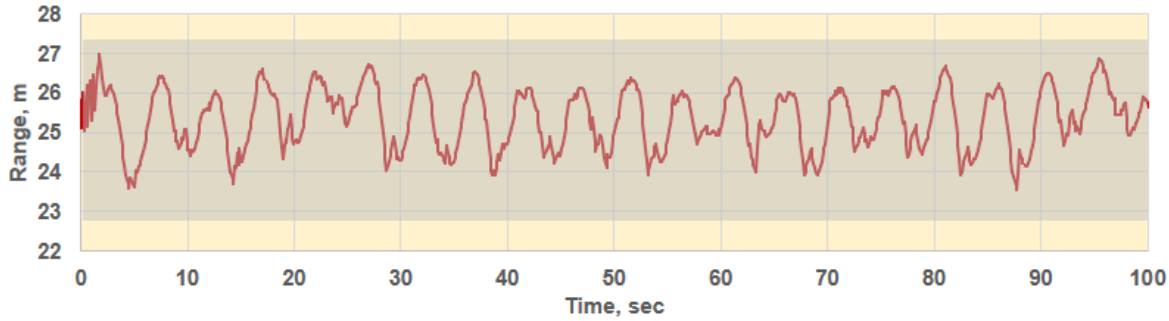

(c) Range versus time using a 6 in. hemisphere and Variance = 0.2.
Figure 8. Continued.

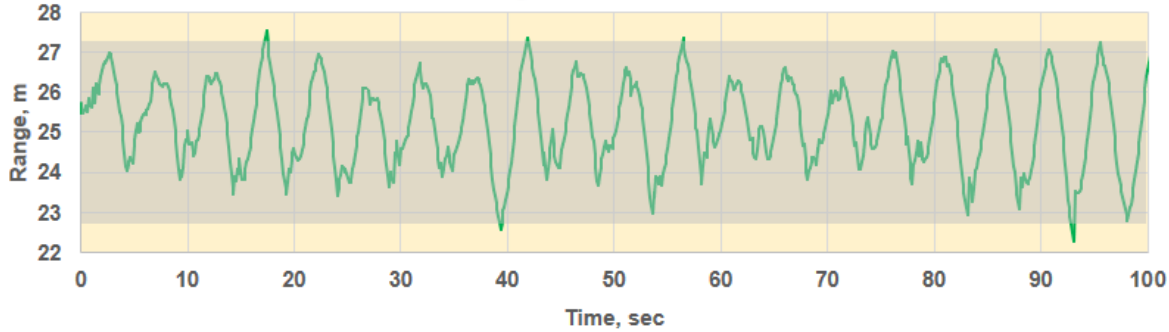

(d) Range versus time using a 6 in. hemisphere and Variance = 0.5.
Figure 8. Continued.

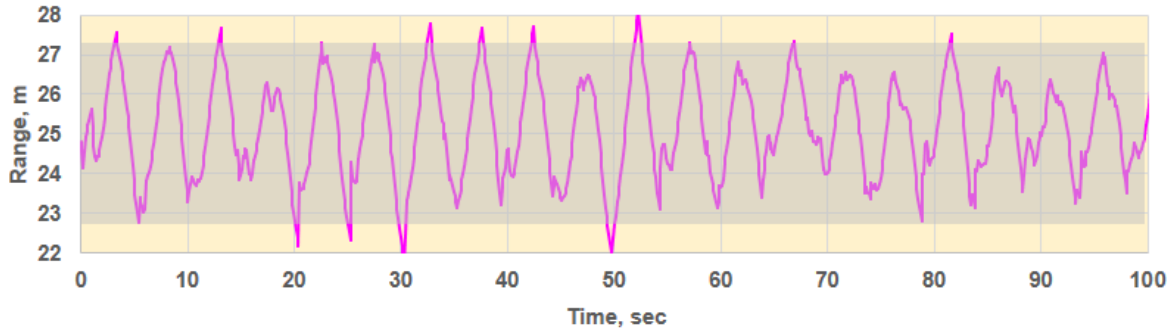

(e) Range versus time using a 6 in. hemisphere and Variance = 1.0.
Figure 8. Continued.

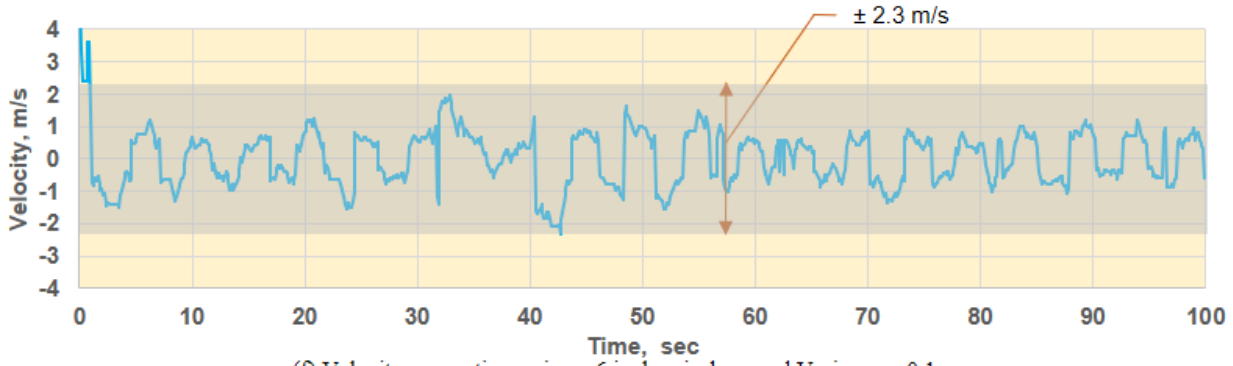

(f) Velocity versus time using a 6 in. hemisphere and Variance = 0.1.
Figure 8. Continued.

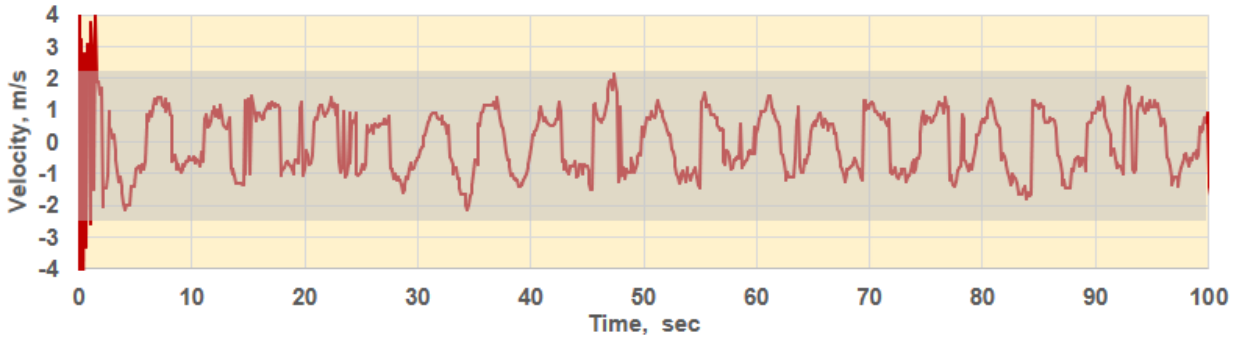

(g) Velocity versus time using a 6 in. hemisphere and Variance = 0.2.
Figure 8. Continued.

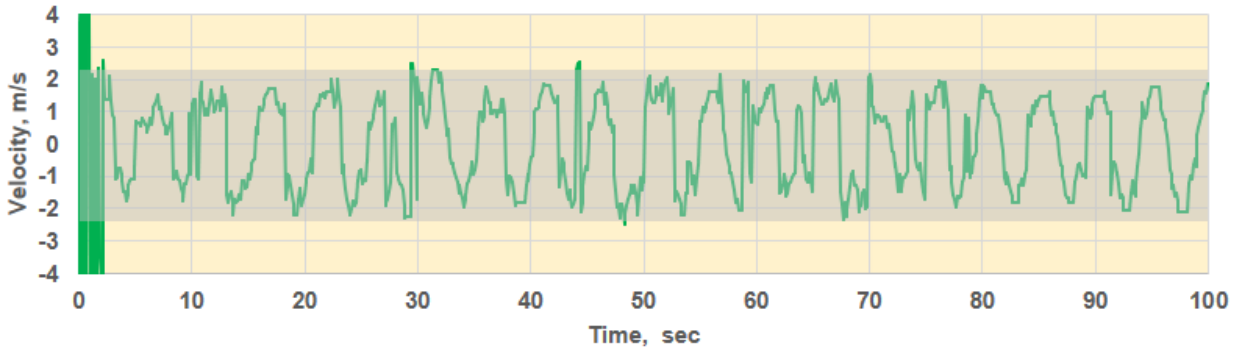

(h) Velocity versus time using a 6 in. hemisphere and Variance = 0.5.
Figure 8. Continued.

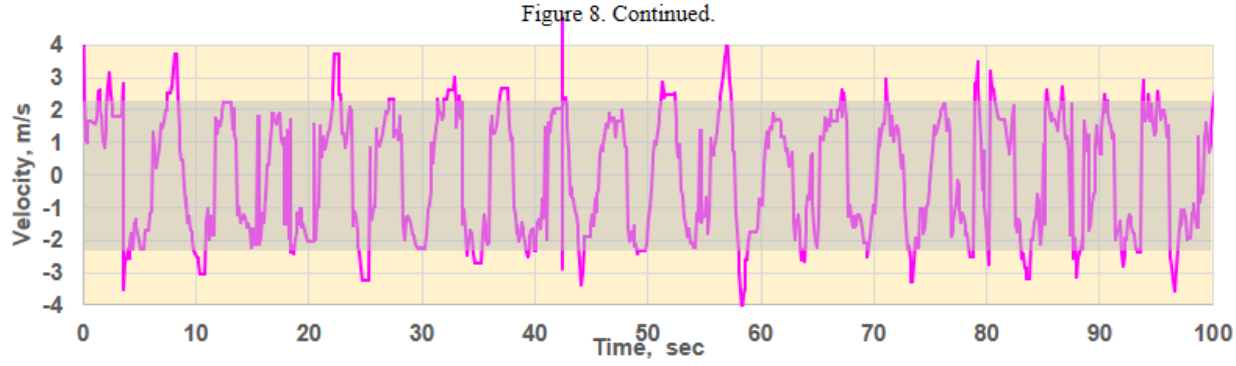

(i) Velocity versus time using a 6 in. hemisphere and Variance = 1.0.
Figure 8. Concluded.

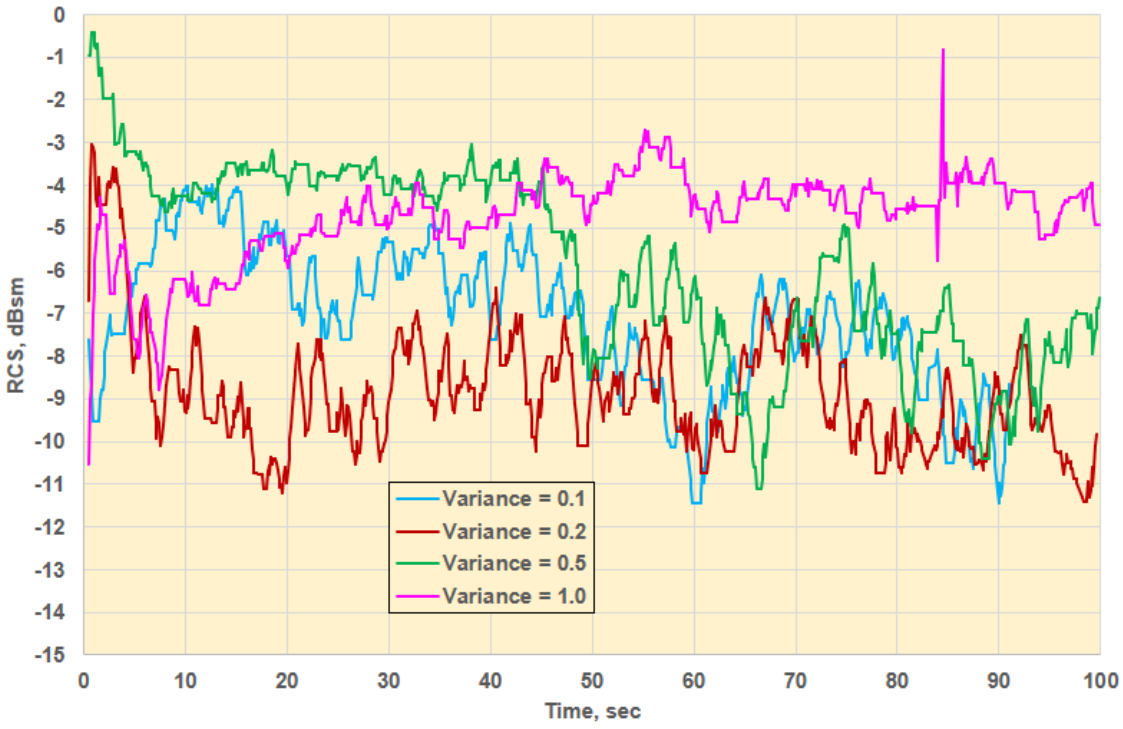

(a) RCS versus time using a 3 in. hemisphere.

Figure 9. Track data measurements for a 3 in. hemisphere with variance settings of 0.1, 0.2, 0.5, and 1.0.

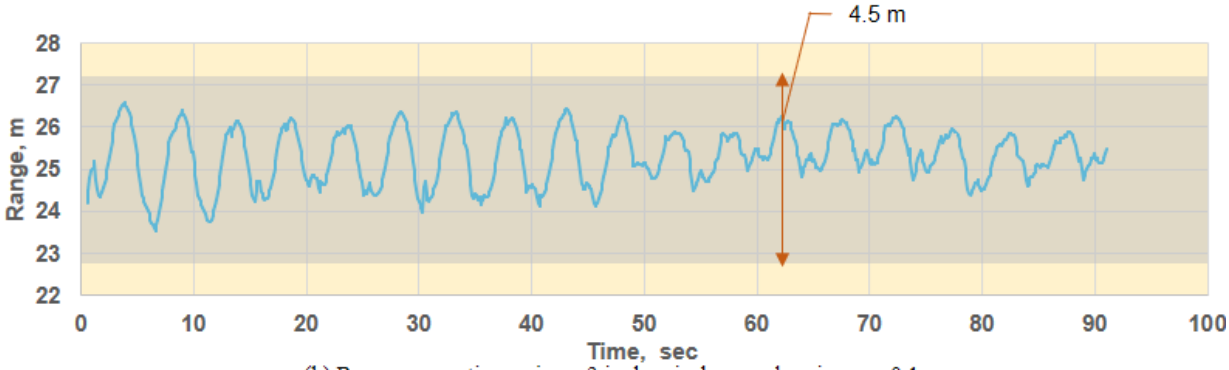

(b) Range versus time using a 3 in. hemisphere and variance = 0.1.
Figure 9. Continued.

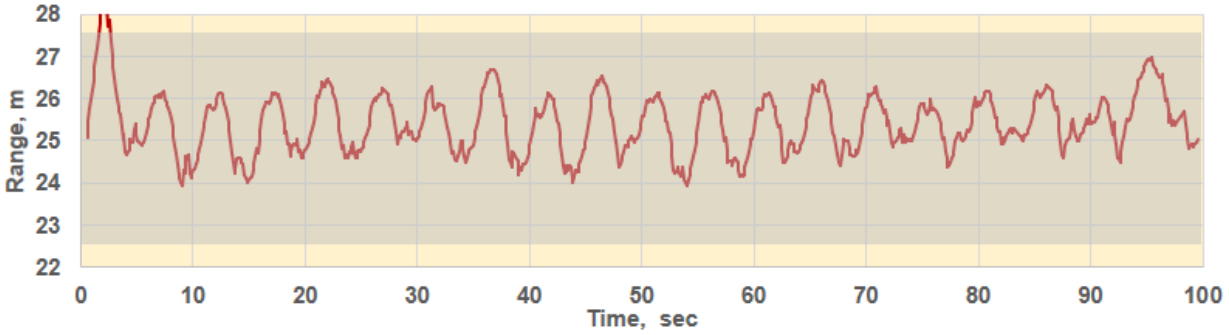

(c) Range versus time using a 3 in. hemisphere and variance = 0.2.
Figure 9. Continued.

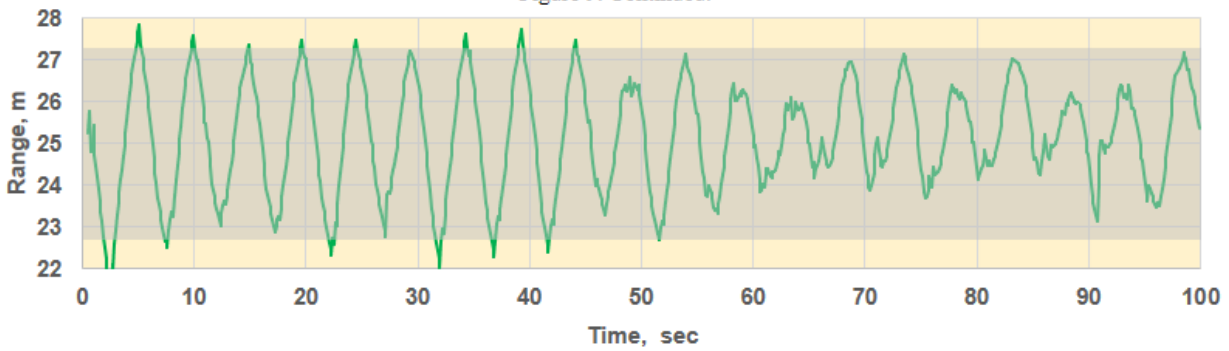

(d) Range versus time using a 3 in. hemisphere and variance = 0.5.
Figure 9. Continued.

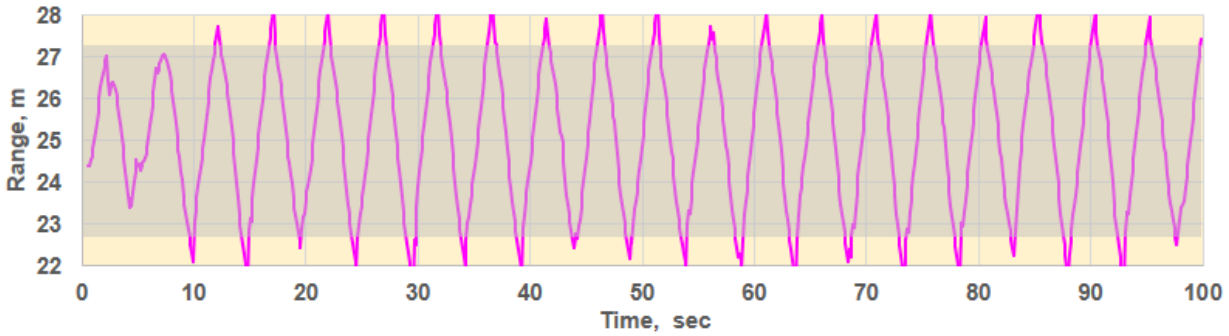

(e) Range versus time using a 3 in. hemisphere and variance = 1.0.
Figure 9. Continued.

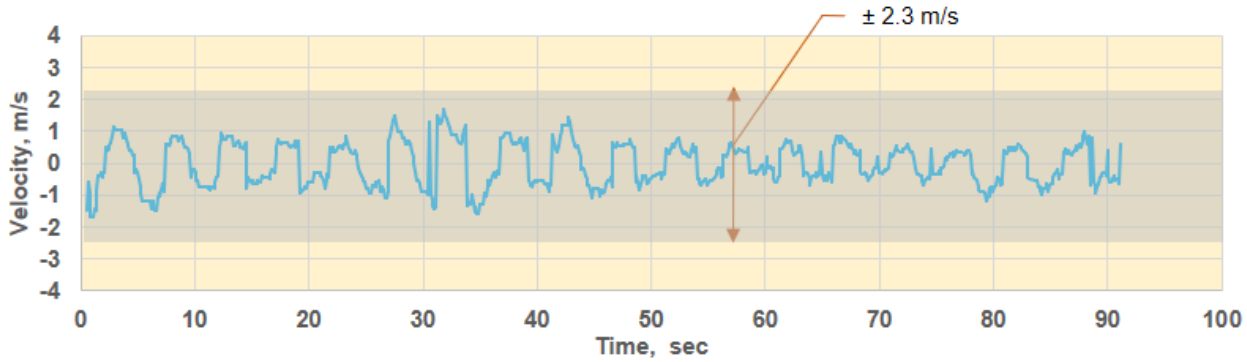

(f) Velocity versus time using a 3 in. hemisphere and variance = 0.1.
Figure 9. Continued.

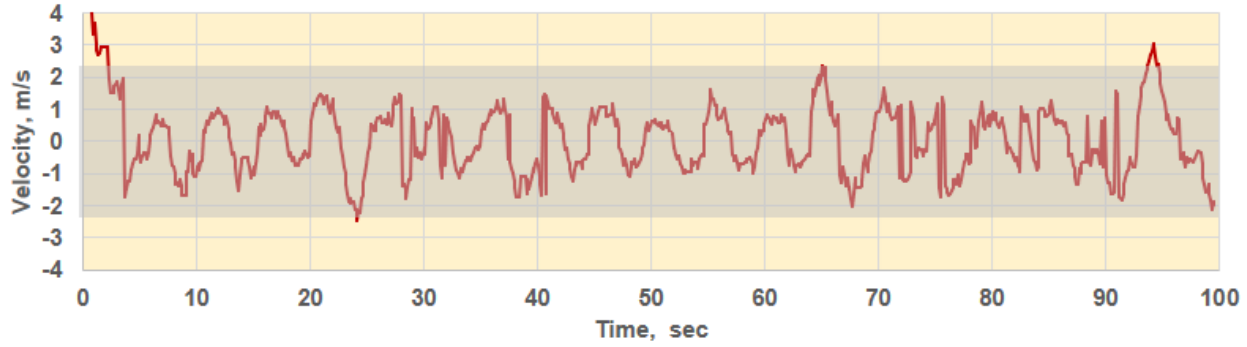

(g) Velocity versus time using a 3 in. hemisphere and variance = 0.2.
Figure 9. Continued.

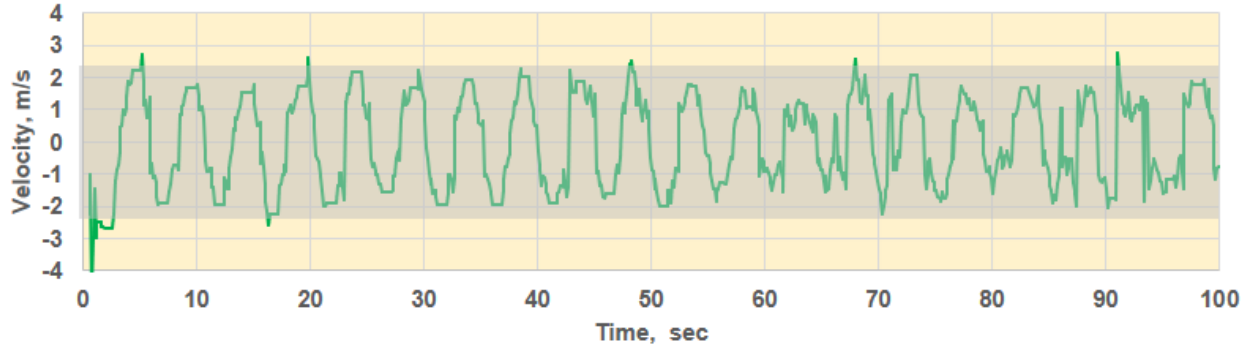

(h) Velocity versus time using 3 in. hemisphere and variance = 0.5.
Figure 9. Continued.

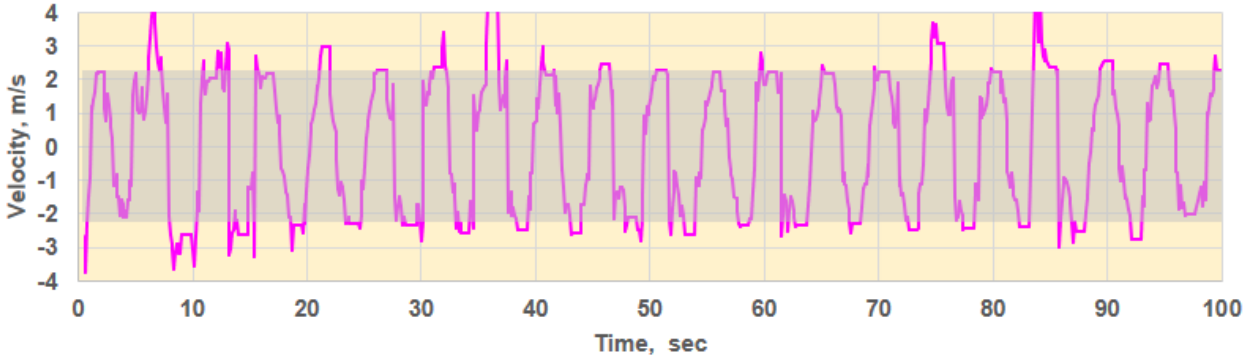

(i) Velocity versus time using a 3 in. hemisphere and variance = 1.0.
Figure 9. Concluded.

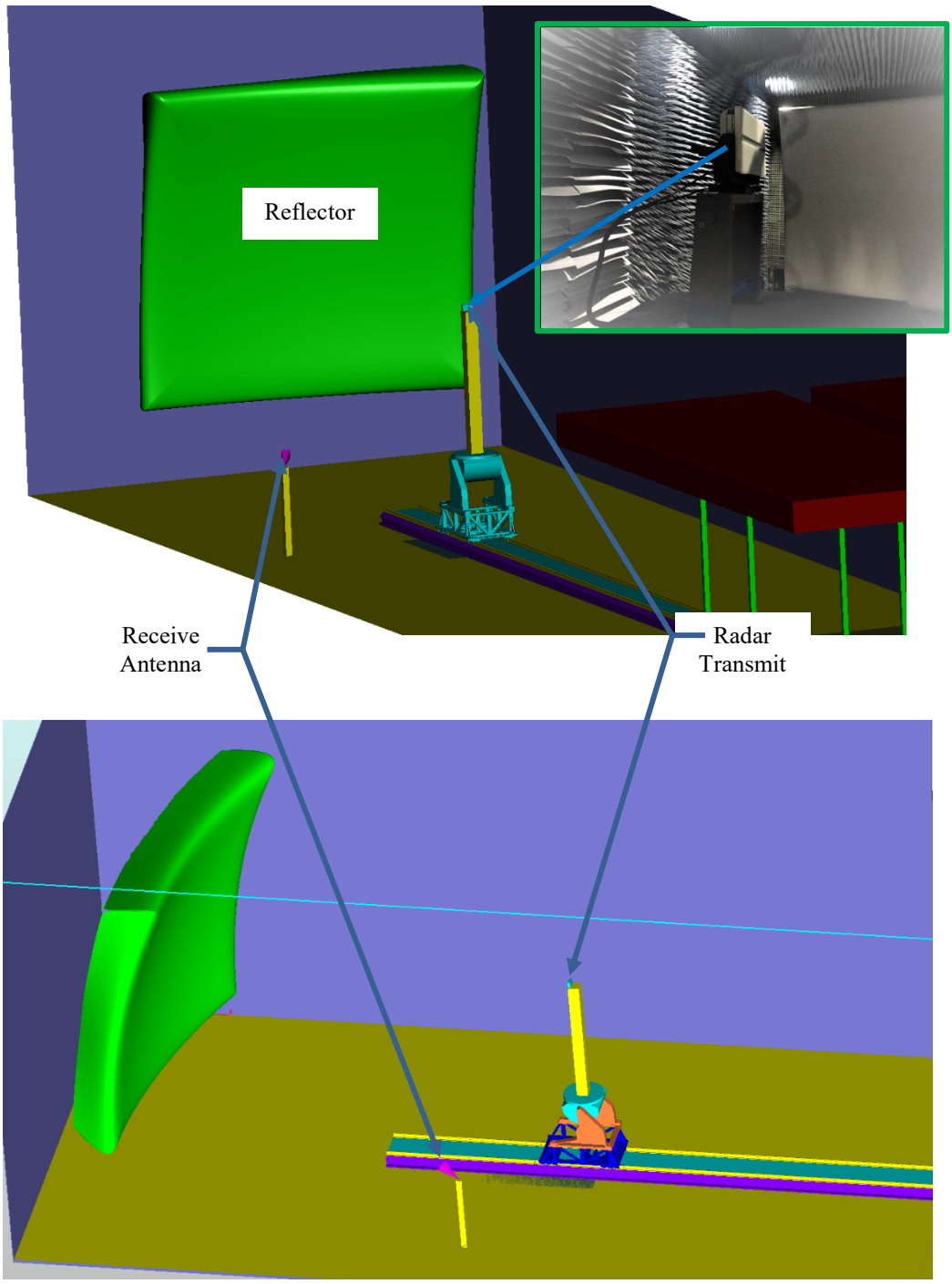

Figure 10. Radar antenna pattern acquisition setup.

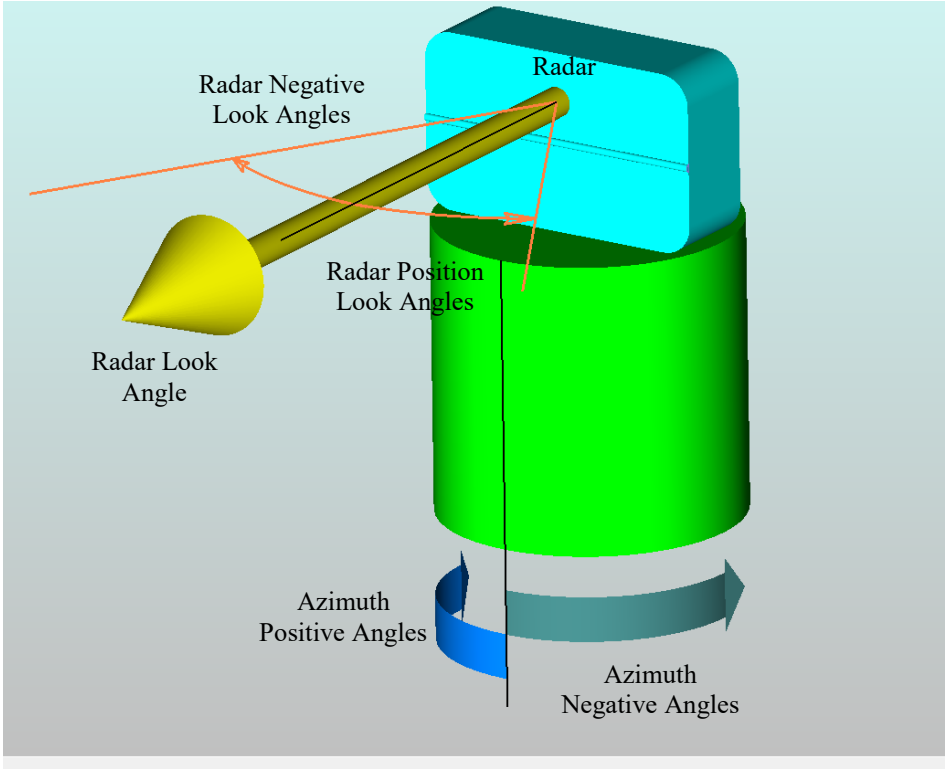

Figure 11. E plane setup and radar look angle coordinate system for azimuth cuts.

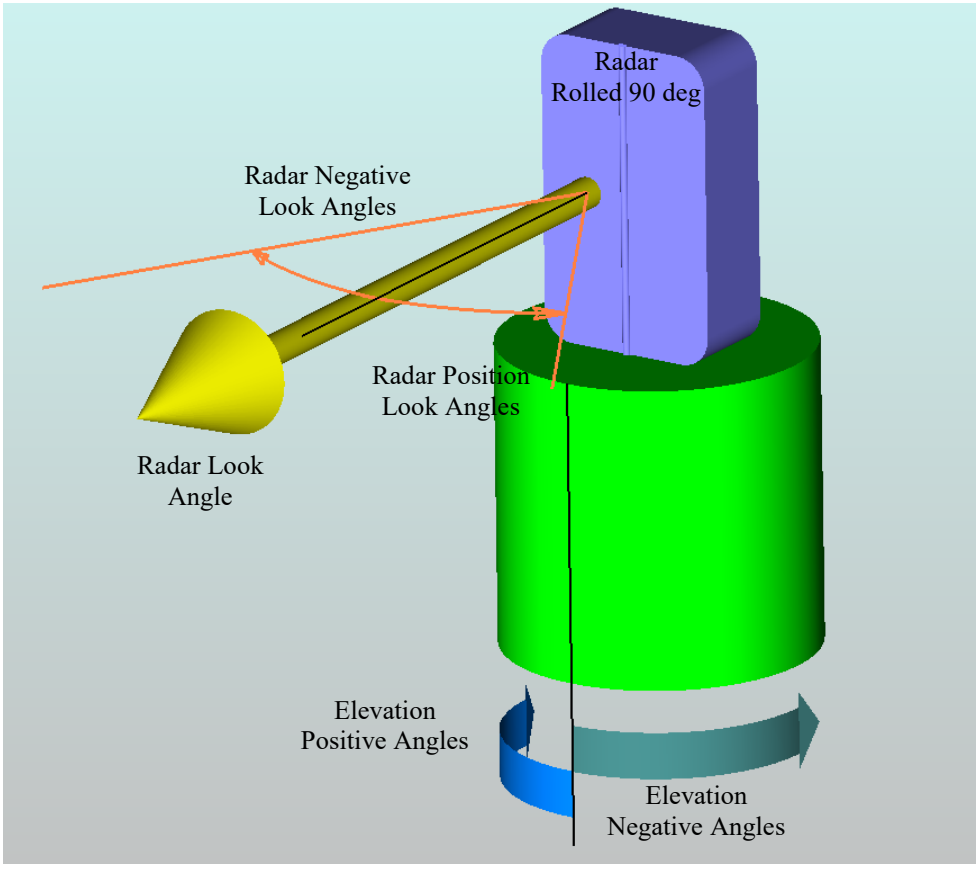

Figure 12. H plane setup and radar look angle coordinate system for elevation cuts.

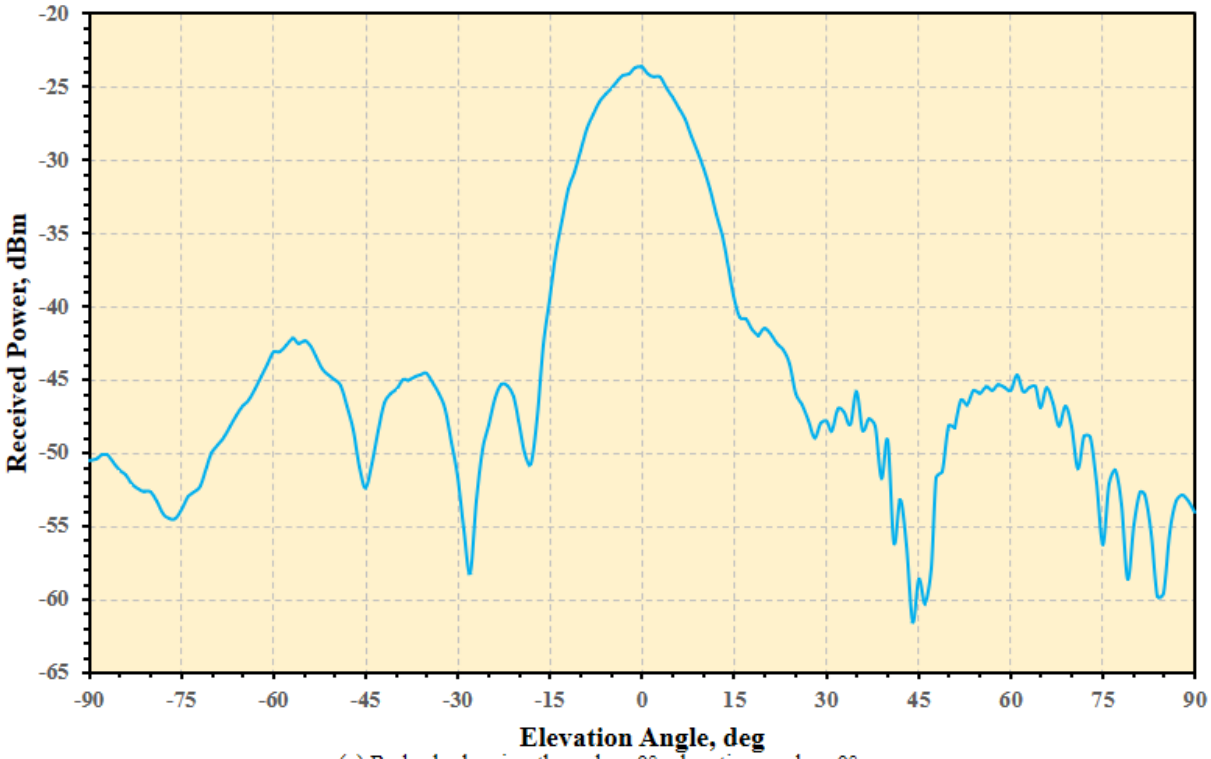

(a) Radar look azimuth angle = 0°, elevation angle = 0°.

Figure 13. Radar transmit antenna pattern in H-Plane.

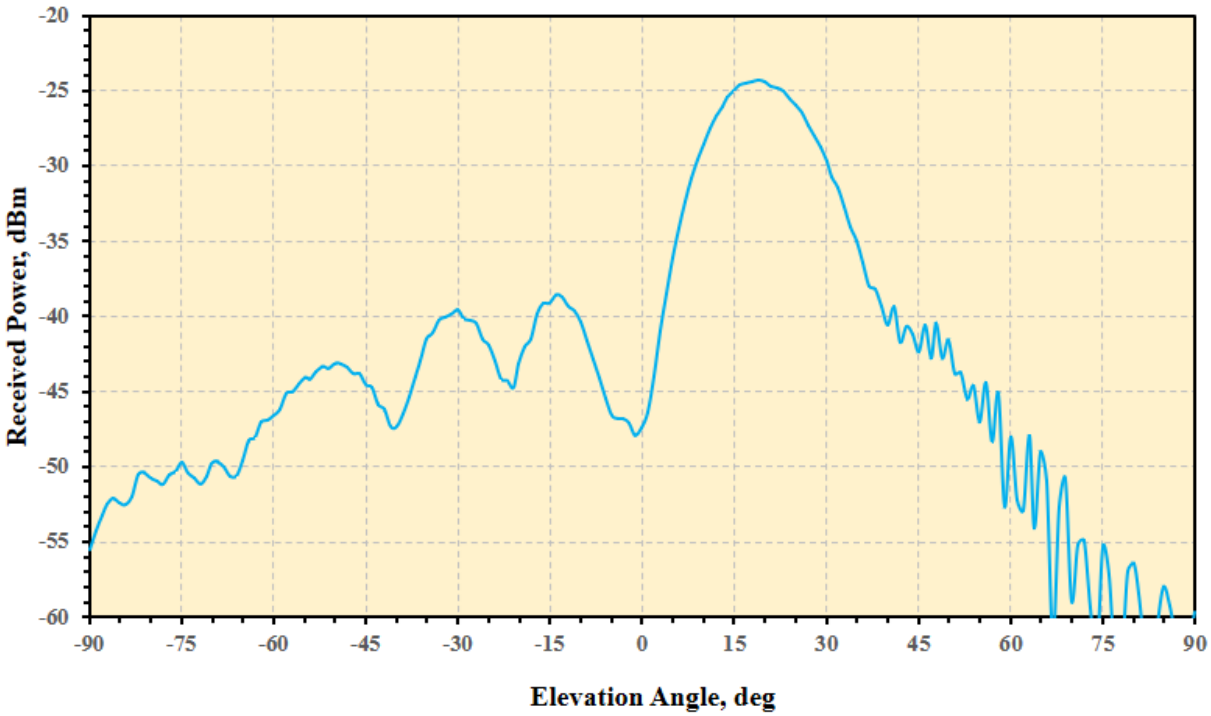

(b) Radar look azimuth angle = 0°, elevation angle = -20°.

Figure 13. Continued.

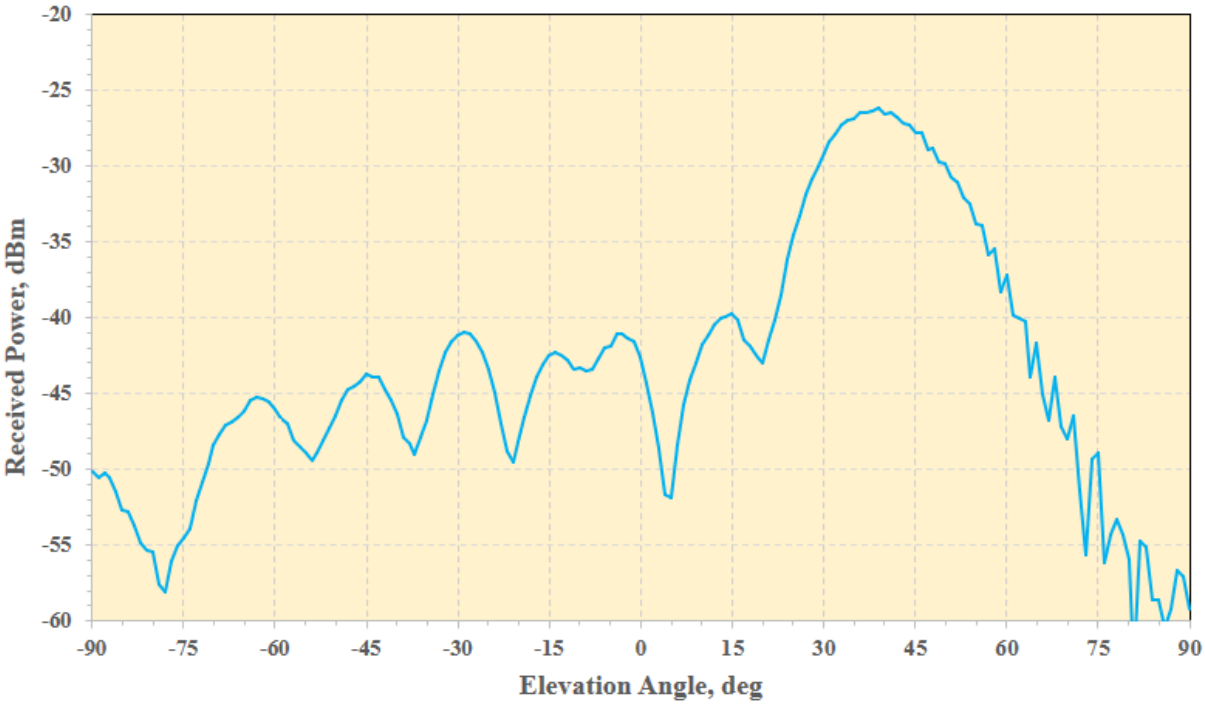

(b) Radar look azimuth angle = 0°, elevation angle = -40°.
Figure 13. Continued.

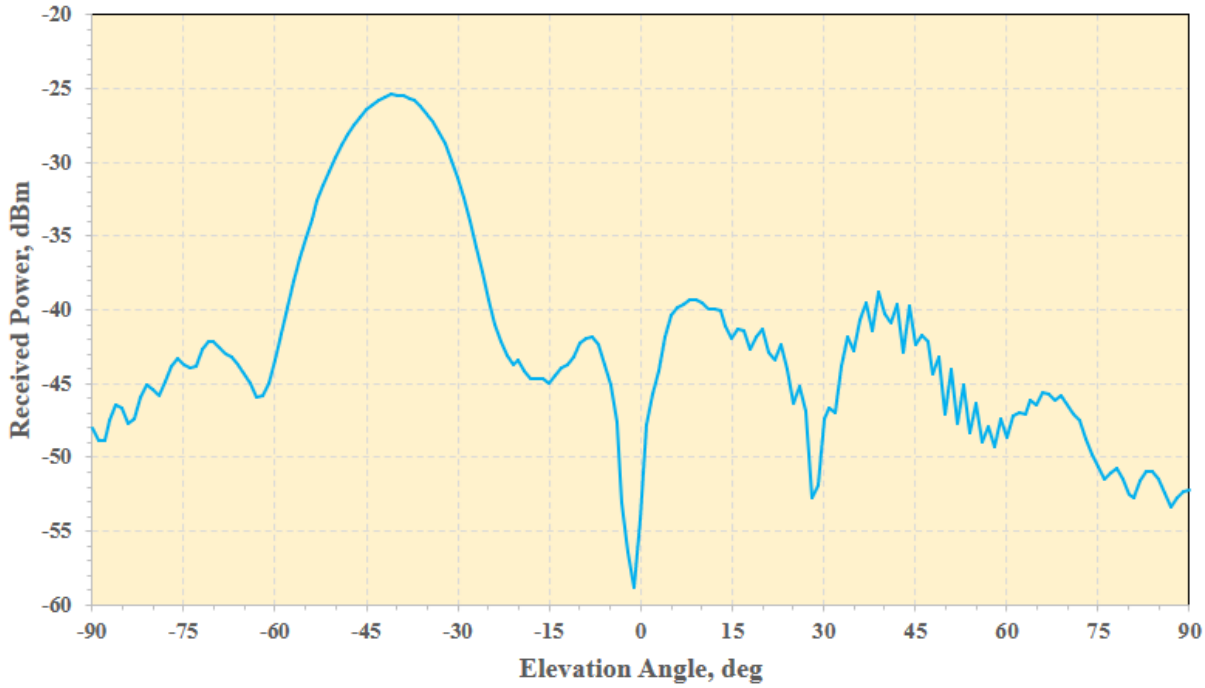

(d) Radar look azimuth angle = 0°, elevation angle = +40°.
Figure 13. Concluded.

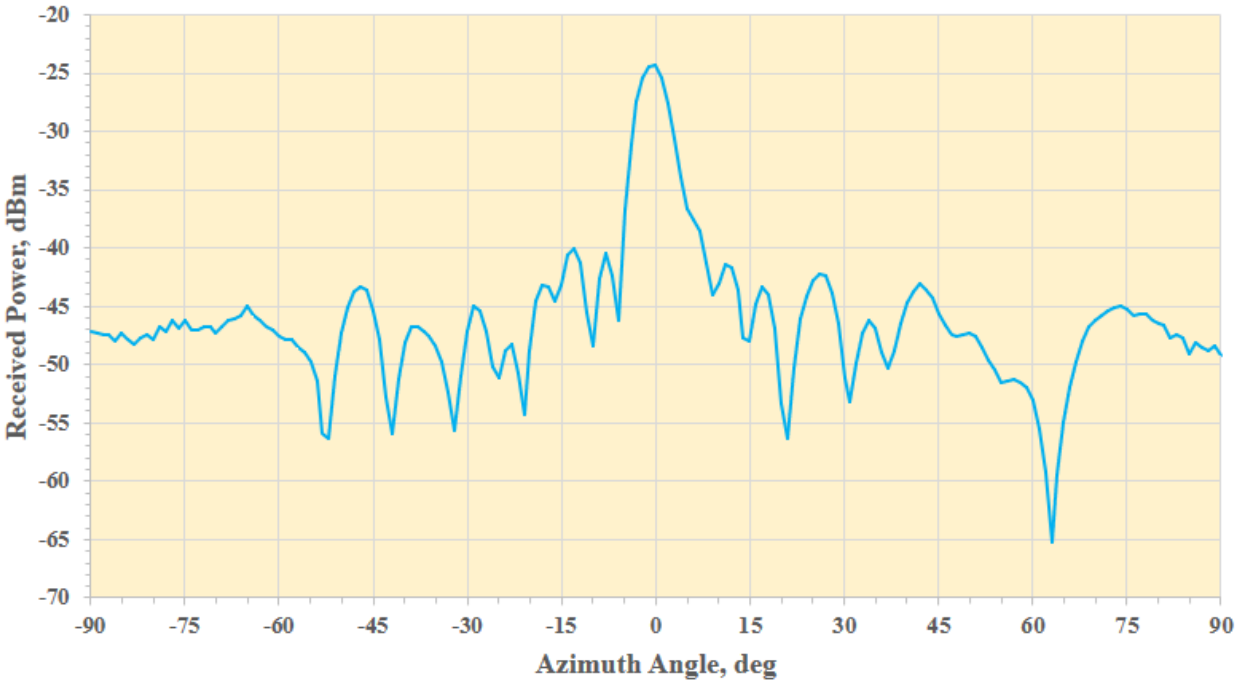

(a) Radar look azimuth angle = 0°, elevation angle = 0°.
Figure 14. Radar transmit antenna pattern in E-Plane.

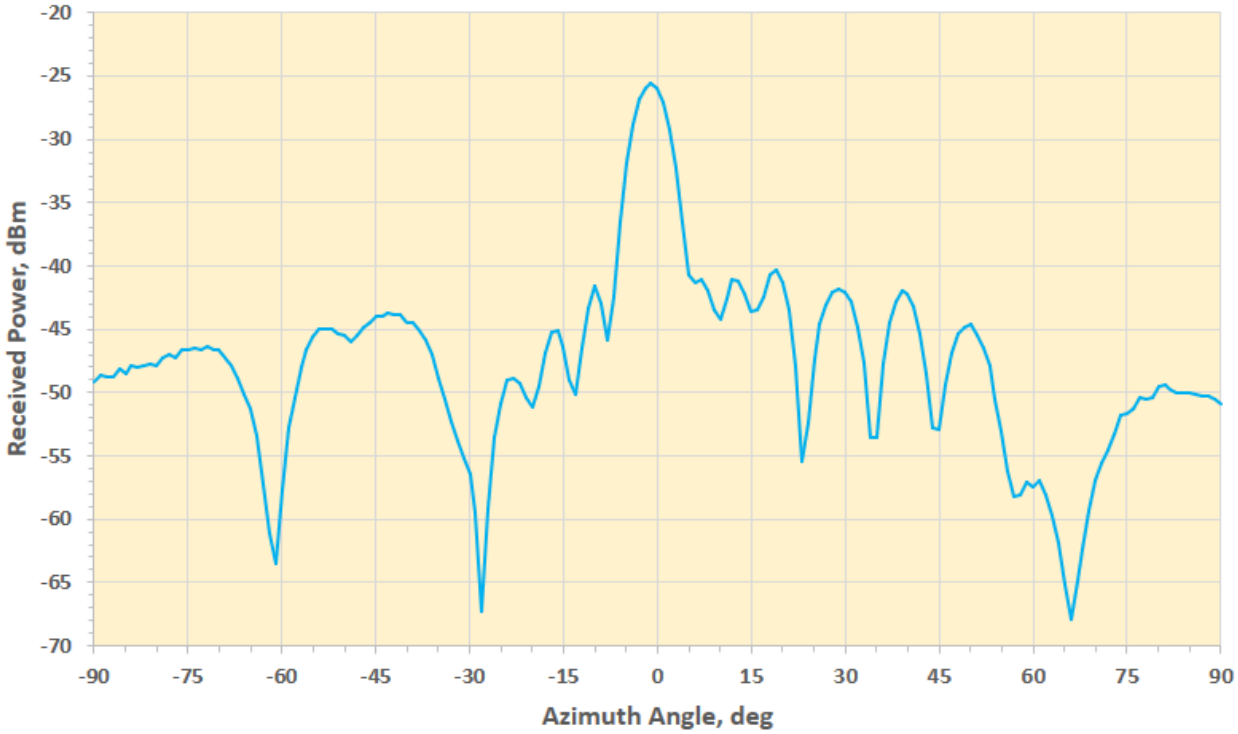

(b) Radar look azimuth angle = 0°, elevation angle = +40°.
Figure 14. Concluded.

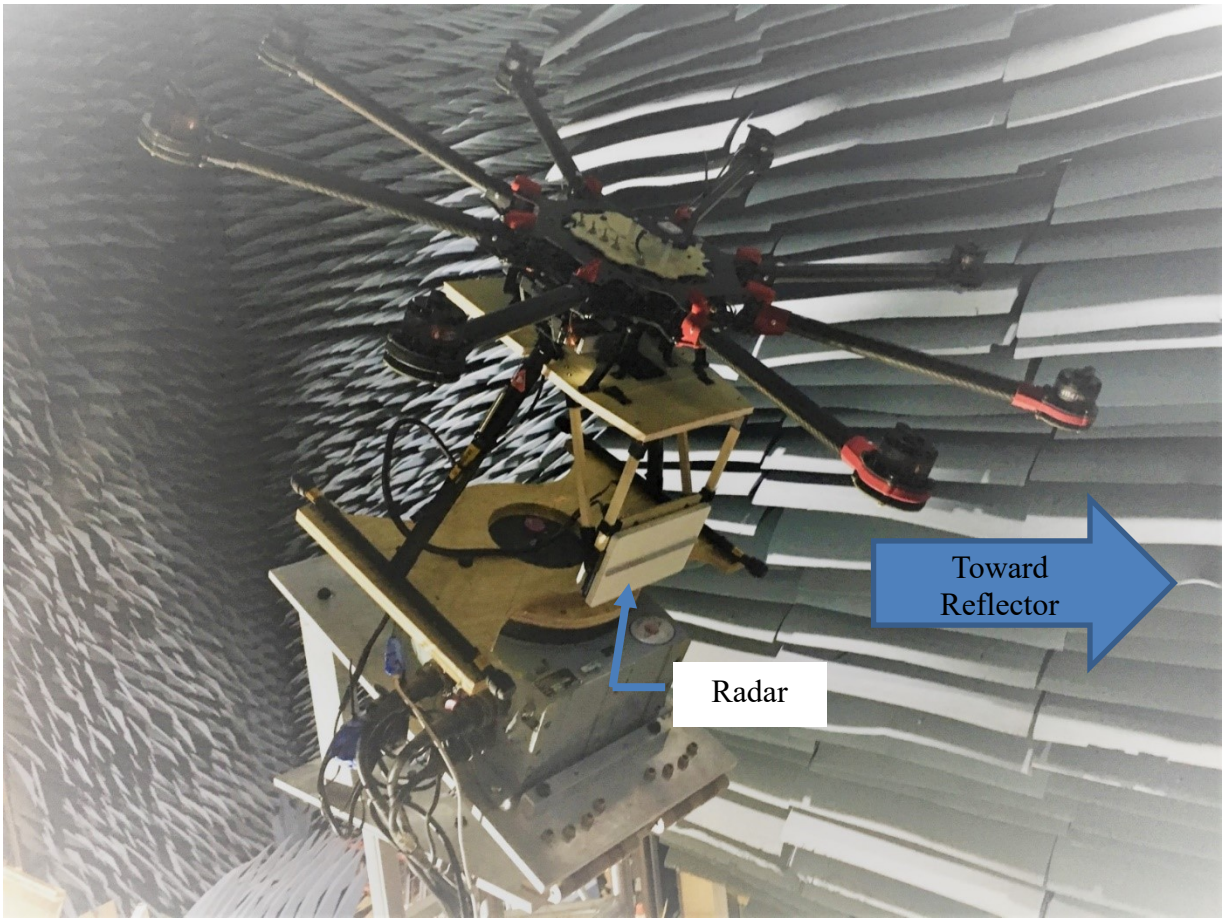

Figure 15. Radar transmit antenna pattern setup installed on a UAS.

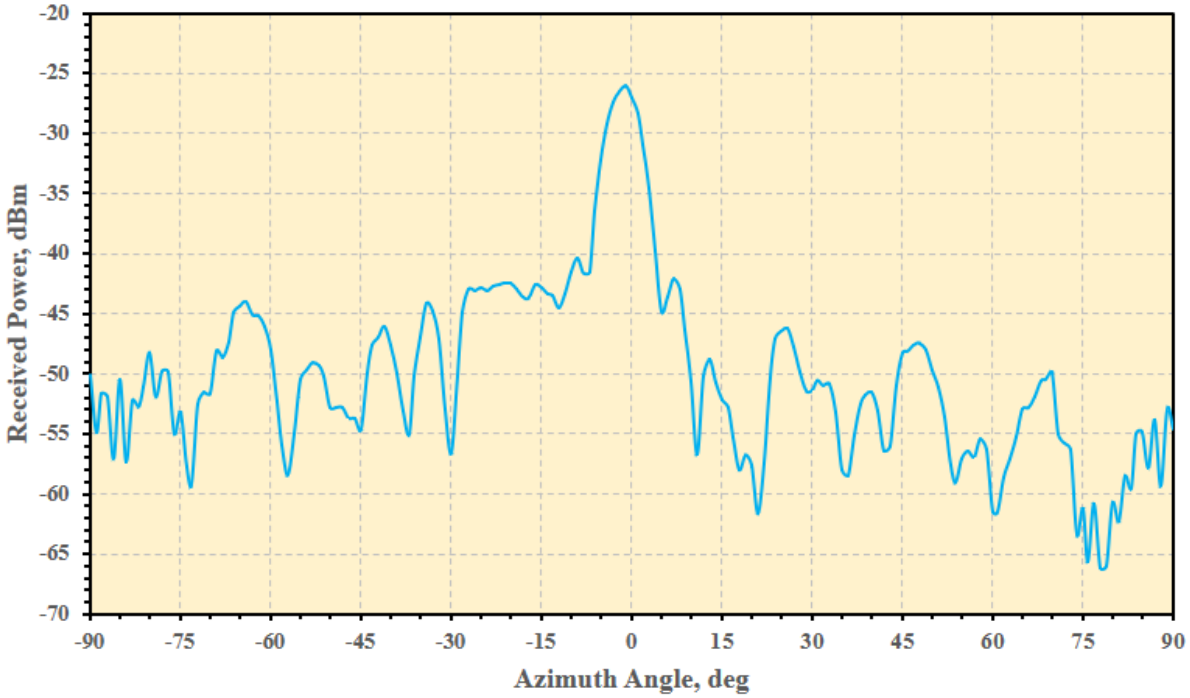

(a) Radar look azimuth angle = 0°, elevation angle = +40°.
Figure 16. Radar transmit antenna pattern in E-Plane with radar installed on a UAS.

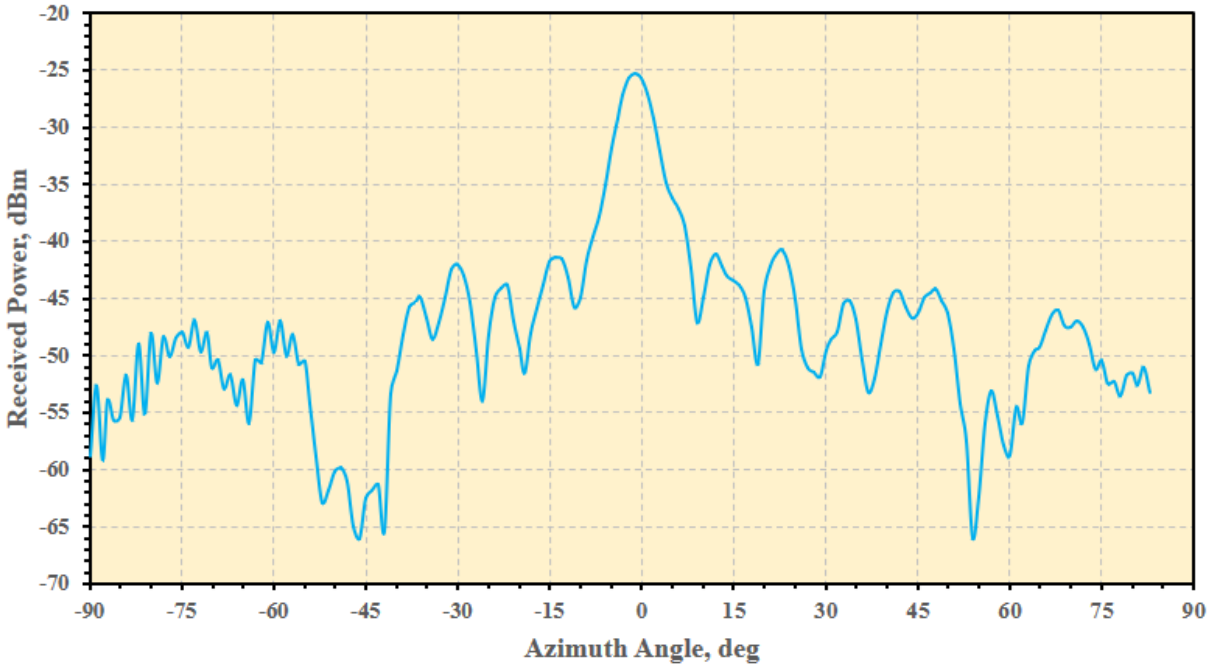

(b) Radar look azimuth angle = 0°, elevation angle = +30°.
Figure 16. Continued.

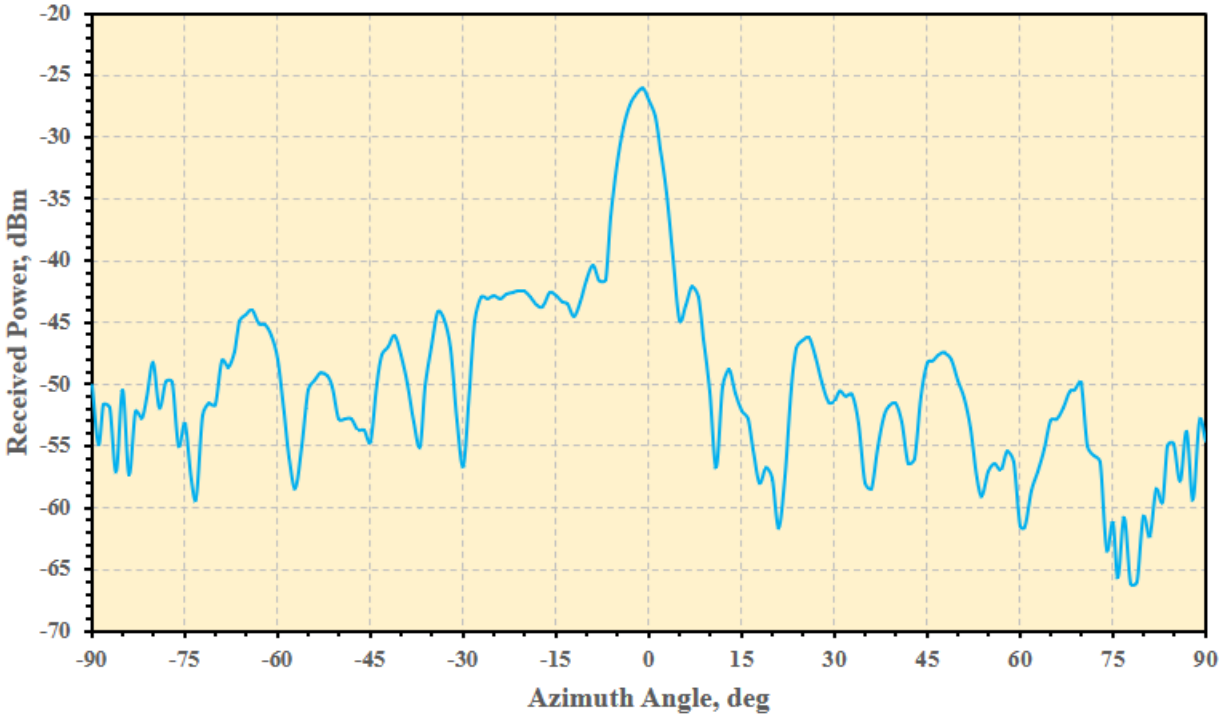

(a) Radar look azimuth angle = 0°, elevation angle = +40°.

Figure 16. Radar transmit antenna pattern in E-Plane with radar installed on a UAS.

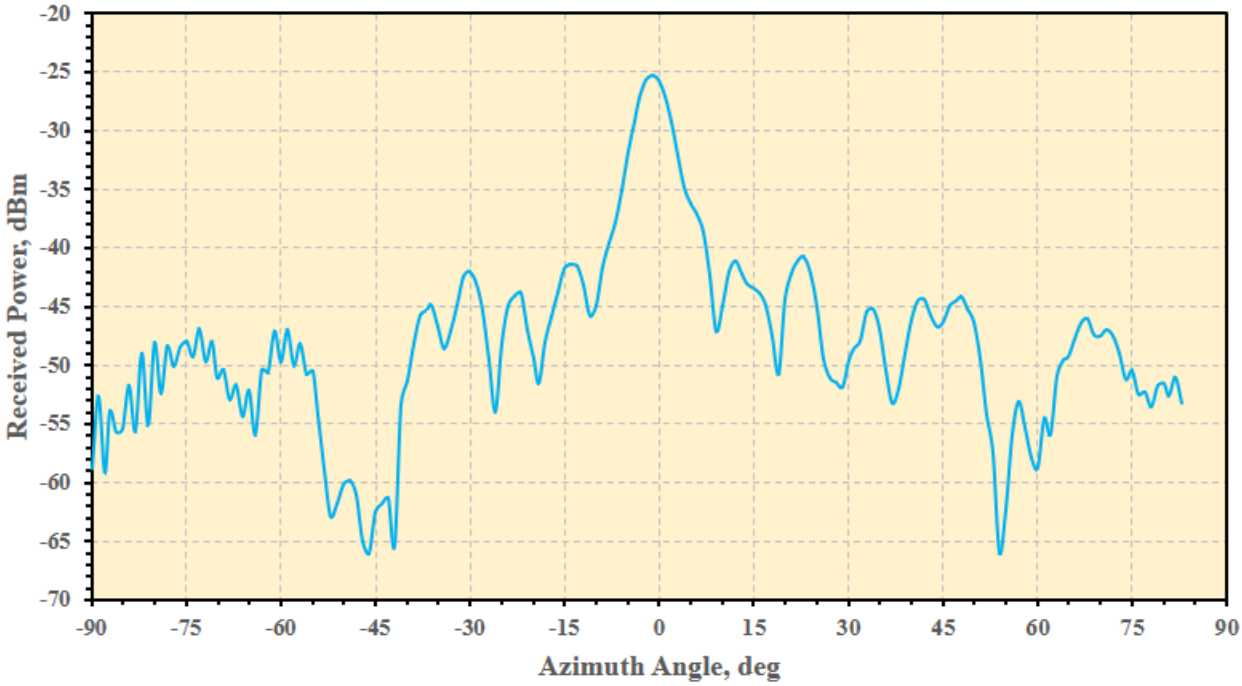

(b) Radar look azimuth angle = 0°, elevation angle = +30°.

Figure 16. Continued.

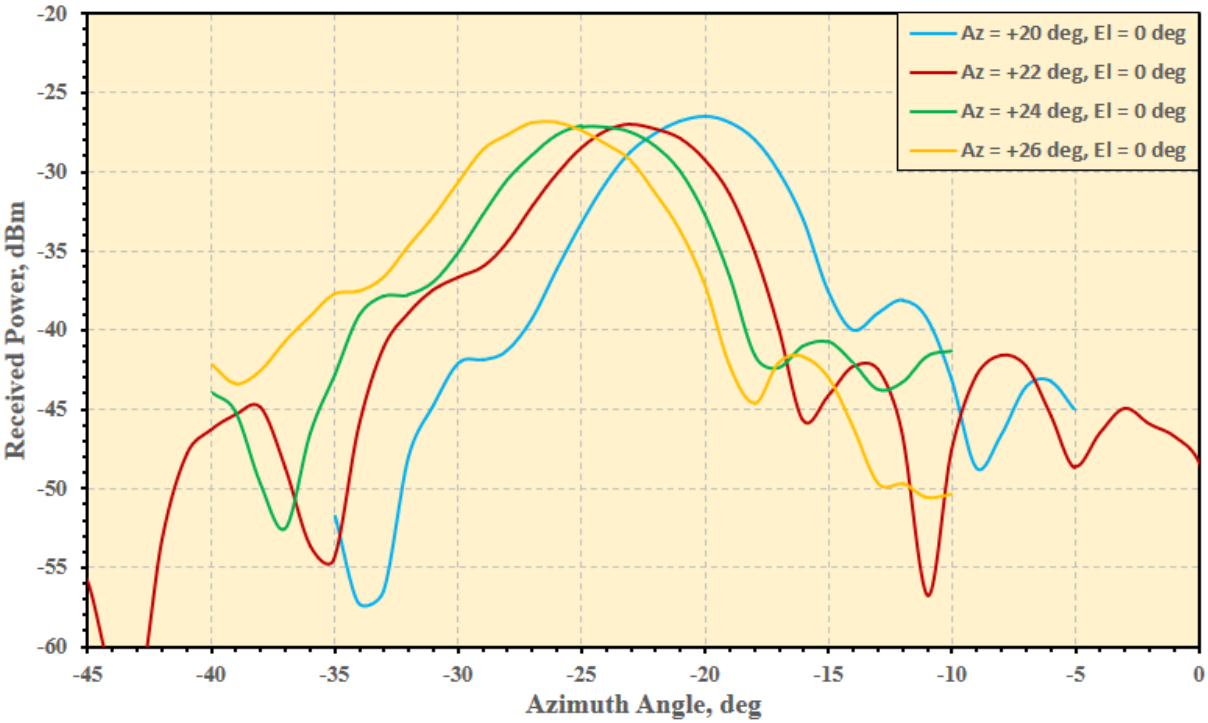

Figure 17. Radar transmit antenna pattern in E-Plane with radar installed on a UAS with radar look azimuth angles = 20°, 22°, 24°, 26° and elevation angle = 0°.

REPORT DOCUMENTATION PAGE

Form Approved
OMB No. 0704-0188

1. REPORT DATE *(DD-MM-YYYY)*
1-05-2019

2. REPORT TYPE
Technical Memorandum

3. DATES COVERED *(From - To)*

4. TITLE AND SUBTITLE
Indoor Ground Testing of a Small UAS Sense and Avoid Airborne Doppler Radar

5a. CONTRACT NUMBER

5b. GRANT NUMBER

5c. PROGRAM ELEMENT NUMBER

6. AUTHOR(S)
Szatkowski, George N.; Ticatch, Larry A.; Morris, Christopher M.; Cavone, Angelo A.

5d. PROJECT NUMBER

5e. TASK NUMBER

5f. WORK UNIT NUMBER
334005.05.10.07.01

7. PERFORMING ORGANIZATION NAME(S) AND ADDRESS(ES)
NASA Langley Research Center
Hampton, VA 23681-2199

8. PERFORMING ORGANIZATION REPORT NUMBER
L-21021

9. SPONSORING/MONITORING AGENCY NAME(S) AND ADDRESS(ES)
National Aeronautics and Space Administration
Washington, DC 20546-0001

10. SPONSOR/MONITOR'S ACRONYM(S)
NASA

11. SPONSOR/MONITOR'S REPORT NUMBER(S)
NASA-TM-2019-220280

12. DISTRIBUTION/AVAILABILITY STATEMENT
Unclassified-
Subject Category 03
Availability: NASA STI Program (757) 864-9658

13. SUPPLEMENTARY NOTES

14. ABSTRACT The National Aeronautics and Space Administration's Unmanned Aircraft System (UAS) Traffic Management (UTM) project is researching prototype technologies needed to ensure safe integration of UAS operations into the National Airspace System (NAS). Within the UTM Concept of Operations, UAS would be equipped with on-board Sense and Avoid (SAA) technology to continually monitor for manned and unmanned aircraft in its vicinity while operating beyond visual line of sight in uncontrolled airspace. To support this effort, a candidate commercially available 24.5 GHz Doppler radar was selected and evaluated to determine if the technology could reliably support minimum requirements for SAA applications of small UAS (sUAS). Indoor ground tests were conducted inside the NASA Langley Research Center's Experimental Test Range (ETR) from a stationary platform to evaluate the Doppler radar performance characteristics and gain operational proficiency before the radar was authorized to transmit outdoors. A high speed linear rail system was developed for the radar evaluation and was shown to be an effective method to generate Doppler radar targets of known radar cross section. The accuracy of the range and velocity reported by the radar was shown to be dependent on the Kalman filter state variance parameter settings.

15. SUBJECT TERMS
Antenna Measurements; Doppler radar; Experimental Test Range; ICAROUS; sUAS

16. SECURITY CLASSIFICATION OF:			17. LIMITATION OF ABSTRACT	18. NUMBER OF PAGES	19a. NAME OF RESPONSIBLE PERSON
a. REPORT	b. ABSTRACT	c. THIS PAGE			STI Help Desk (email: help@sti.nasa.gov)
U	U	U	UU	41	19b. TELEPHONE NUMBER *(Include area code)* (757) 864-9658